

# Ultra-high Energy Neutrinos and Cosmic Rays as Probes of New Physics

G. Sigl\*

*Institut d'Astrophysique de Paris, C.N.R.S., 98 bis boulevard Arago, F-75014 Paris, France*

October 31, 2018

## Abstract

Cosmic high energy neutrinos are inextricably linked to the origin of cosmic rays which is one of the major unresolved questions in astrophysics. In particular, the highest energy cosmic rays observed possess macroscopic energies and their origin is likely to be associated with the most energetic processes in the Universe. Their existence triggered a flurry of theoretical explanations ranging from conventional shock acceleration to particle physics beyond the Standard Model and processes taking place at the earliest moments of our Universe. Furthermore, many new experimental activities promise a considerable increase of statistics at the highest energies and a combination with  $\gamma$ -ray and neutrino astrophysics will put strong constraints on these theoretical models. The detection of ultra high energy neutrinos in particular is made likely by new experimental techniques and will open an important new channel. We give an overview over this quickly evolving field with special emphasis on new experimental ideas and possibilities for probing new physics beyond the electroweak scale.

---

\*sigl@iap.fr

# Contents

<b>1</b>	<b>Introduction</b>	<b>1</b>
<b>2</b>	<b>Present and Future UHE CR and Neutrino Experiments</b>	<b>4</b>
<b>3</b>	<b>Neutrino Interactions and Propagation</b>	<b>6</b>
3.1	Neutrino propagation . . . . .	6
3.2	Neutrino detection . . . . .	10
3.3	New Interactions . . . . .	12
<b>4</b>	<b>Top-Down Scenarios</b>	<b>15</b>
4.1	The Main Idea . . . . .	15
4.2	Numerical Simulations . . . . .	17
4.3	Results: $\gamma$ -ray and Nucleon Fluxes . . . . .	19
4.4	Results: Neutrino Fluxes . . . . .	21
<b>5</b>	<b>Conclusions</b>	<b>24</b>
	<b>References</b>	<b>25</b>

# 1 Introduction

The furthest continuous source so far observed in neutrinos is the Sun [1]. These solar neutrinos together with their atmospheric cousins [2, 3] which are produced by cosmic ray interactions in the atmosphere have in fact provided evidence for neutrino mass and oscillations. They are thus playing an important role in probing new physics beyond the Standard Model. The only extragalactic source so far observed in neutrinos in the 10 MeV range was sporadic, namely supernova 1987A. These neutrinos have extensively been used to constrain neutrino masses and oscillation parameters [4].

Neutrinos at much higher energies, above a GeV or so, have not been detected yet due to the small fluxes and cross sections. However, the disadvantage of difficult detection is at the same time a blessing because it makes these elusive particles reach us unattenuated over cosmological distances and from very dense environments where all other particles (except gravitational waves) would be absorbed. Such neutrinos are expected to be produced, apart from more speculative mechanisms such as decay of superheavy particles, as secondary products of interactions of the well known cosmic rays in extragalactic and galactic sources as well as during propagation. These high energy neutrinos are therefore inextricably linked with the physics and astrophysics of cosmic rays. These lectures will therefore discuss high energy neutrinos together with cosmic rays. The main focus will thereby be on new possibilities opened by new experimental techniques now under consideration or already under construction, and resulting probes of new physics at very high energies beyond the electroweak scale. We thus begin with a short discussion of the now very active field of ultrahigh energy cosmic rays in general.

After almost 90 years of research on cosmic rays (CRs), their origin is still an open question, for which the degree of uncertainty increases with energy: Only below 100 MeV kinetic energy, where the solar wind shields protons coming from outside the solar system, the sun must give rise to the observed proton flux. The bulk of the CRs up to at least an energy of  $E = 4 \times 10^{15}$  eV is believed to originate within our Galaxy. Above that energy, which is associated with the so called “knee”, the flux of particles per area, time, solid angle, and energy, which can be well approximated by broken power laws  $\propto E^{-\gamma}$ , steepens from a power law index  $\gamma \simeq 2.7$  to one of index  $\simeq 3.2$ . Above the so called “ankle” at  $E \simeq 5 \times 10^{18}$  eV, the spectrum flattens again to a power law of index  $\gamma \simeq 2.8$ . This latter feature is often interpreted as a cross over from a steeper Galactic component to a harder component of extragalactic origin. Fig. 1 shows the measured CR spectrum above 100 MeV, up to  $3 \times 10^{20}$  eV, the highest energy measured so far for an individual CR.

The conventional scenario assumes that all high energy charged particles are accelerated in magnetized astrophysical shocks, whose size and typical magnetic field strength determines the maximal achievable energy, similar to the situation in man made particle accelerators. The most likely astrophysical accelerators for CR up to the knee, and possibly up to the ankle are the shocks associated with remnants of past Galactic supernova explosions, whereas for the presumed extragalactic component powerful objects such as active galactic nuclei are envisaged.

The main focus of this contribution will be on ultrahigh energy cosmic rays (UHECRs), those with energy  $\gtrsim 10^{18}$  eV [6, 7, 8, 11, 12, 13], see Fig. 2, and neutrinos in the same energy

range, which have not been detected yet. For more details on CRs in general the reader is referred to recent monographs [14, 15]. In particular, extremely high energy (EHE)<sup>1</sup> cosmic rays pose a serious challenge for conventional theories of CR origin based on acceleration of charged particles in powerful astrophysical objects. The question of the origin of these EHECRs is, therefore, currently a subject of much intense debate and discussions as well as experimental efforts; for a short review for the non-experts see Ref. [16], for recent brief reviews see Ref. [17, 18] and for a detailed review see Ref. [19]. In Sect. 2 we will summarize detection techniques and present and future experimental projects.

The current theories of origin of EHECRs can be broadly categorized into two distinct “scenarios”: the “bottom-up” acceleration scenario, and the “top-down” decay scenario, with various different models within each scenario. As the names suggest, the two scenarios are in a sense exact opposite of each other. The bottom-up scenario is just an extension of the conventional shock acceleration scenario in which charged particles are accelerated from lower energies to the requisite high energies in certain special astrophysical environments. On the other hand, in the top-down scenario, the energetic particles arise simply from decay of certain sufficiently massive particles originating from physical processes in the early Universe, and no acceleration mechanism is needed.

The problems encountered in trying to explain EHECRs in terms of acceleration mechanisms have been well-documented in a number of studies; see, e.g., Refs. [20, 21, 22]. Even if it is possible, in principle, to accelerate particles to EHECR energies of order 100 EeV in some astrophysical sources, it is generally extremely difficult to get the particles come out of the dense regions in and/or around the sources without losing much energy. Currently, the most favorable sources in this regard are perhaps a class of powerful radio galaxies (see, e.g., Refs. [23, 24] for recent reviews and references to the literature), although the values of the relevant parameters required for acceleration to energies  $\gtrsim 100$  EeV are somewhat on the extreme side [22]. However, even if the requirements of energetics are met, the main problem with radio galaxies as sources of EHECRs is that most of them seem to lie at large cosmological distances,  $\gg 100$  Mpc, from Earth. This is a major problem if EHECR particles are conventional particles such as nucleons or heavy nuclei. The reason is that nucleons above  $\simeq 70$  EeV lose energy drastically during their propagation from the source to Earth due to the Greisen-Zatsepin-Kuzmin (GZK) effect [25, 26], namely, photo-production of pions when the nucleons collide with photons of the cosmic microwave background (CMB), the mean-free path for which is  $\sim$  few Mpc [27]. This process limits the possible distance of any source of EHE nucleons to  $\lesssim 100$  Mpc. If the particles were heavy nuclei, they would be photo-disintegrated [28, 29] in the CMB and infrared (IR) background within similar distances. Thus, nucleons or heavy nuclei originating in distant radio galaxies are unlikely to survive with EHECR energies at Earth with any significant flux, even if they were accelerated to energies of order 100 EeV at source. In addition, if cosmic magnetic fields are not close to existing upper limits, EHECRs are not likely to be deflected strongly by large scale cosmological and/or Galactic magnetic fields. Thus, EHECR arrival directions should point back to their sources in the sky and EHECRs may offer us the unique opportunity of doing charged

---

<sup>1</sup>We shall use the abbreviation EHE to specifically denote energies  $E \gtrsim 10^{20}$  eV, while the abbreviation UHE for “Ultra-High Energy” will sometimes be used to denote  $E \gtrsim 1$  EeV, where  $1 \text{ EeV} = 10^{18} \text{ eV}$ . Clearly UHE includes EHE but not vice versa.

particle astronomy. Yet, for the observed EHECR events so far, no powerful sources close to the arrival directions of individual events are found within about 100 Mpc [30, 21]. Very recently, it has been suggested by Boldt and Ghosh [31] that particles may be accelerated to energies  $\sim 10^{21}$  eV near the event horizons of spinning supermassive black holes associated with presently *inactive* quasar remnants whose numbers within the local cosmological Universe (i.e., within a GZK distance of order 50 Mpc) may be sufficient to explain the observed EHECR flux. This would solve the problem of absence of suitable currently *active* sources associated with EHECRs. A detailed model incorporating this suggestion, however, remains to be worked out.

There are, of course, ways to avoid the distance restriction imposed by the GZK effect, provided the problem of energetics is somehow solved separately and provided one allows new physics beyond the Standard Model of particle physics; we shall discuss suggestions based on neutrinos in Sect. 3.

On the other hand, in the top-down scenario, which will be discussed in Sect. 4, the problem of energetics is trivially solved from the beginning. Here, the EHECR particles owe their origin to decay of some supermassive “X” particles of mass  $m_X \gg 10^{20}$  eV, so that their decay products, envisaged as the EHECR particles, can have energies all the way up to  $\sim m_X$ . Thus, no acceleration mechanism is needed. The sources of the massive X particles could be topological defects such as cosmic strings or magnetic monopoles that could be produced in the early Universe during symmetry-breaking phase transitions envisaged in Grand Unified Theories (GUTs). In an inflationary early Universe, the relevant topological defects could be formed at a phase transition at the end of inflation. Alternatively, the X particles could be certain supermassive metastable relic particles of lifetime comparable to or larger than the age of the Universe, which could be produced in the early Universe through, for example, particle production processes associated with inflation. Absence of nearby powerful astrophysical objects such as AGNs or radio galaxies is not a problem in the top-down scenario because the X particles or their sources need not necessarily be associated with any specific active astrophysical objects. In certain models, the X particles themselves or their sources may be clustered in galactic halos, in which case the dominant contribution to the EHECRs observed at Earth would come from the X particles clustered within our Galactic Halo, for which the GZK restriction on source distance would be of no concern.

By focusing primarily on “non-conventional” scenarios involving new particle physics beyond the electroweak scale, we do not wish to give the wrong impression that these scenarios explain all aspects of EHECRs and UHE neutrinos. In fact, essentially each of the specific models that have been studied so far has its own peculiar set of problems. Indeed, the main problem of non-astrophysical solutions of the EHECR problem in general is that they are highly model dependent. On the other hand, it is precisely because of this reason that these scenarios are also attractive — they bring in ideas of new physics beyond the Standard Model of particle physics (such as Grand Unification and new interactions beyond the reach of terrestrial accelerators) as well as ideas of early Universe cosmology (such as topological defects and/or massive particle production in inflation) into the realms of EHECRs where these ideas have the potential to be tested by future EHECR experiments.

The physics and astrophysics of UHECRs is not only intimately linked with the emerging field of neutrino astronomy (for reviews see Refs. [32, 33]), but also with the already estab-

lished field of  $\gamma$ -ray astronomy (for reviews see, e.g., Ref. [34]) which in turn are important subdisciplines of particle astrophysics (for a review see, e.g., Ref. [35]). Indeed, as we shall see, all scenarios of UHECR origin, including the top-down models, are severely constrained by neutrino and  $\gamma$ -ray observations and limits. In turn, this linkage has important consequences for theoretical predictions of fluxes of extragalactic neutrinos above a TeV or so whose detection is a major goal of next-generation neutrino telescopes (see Sect. 2): If these neutrinos are produced as secondaries of protons accelerated in astrophysical sources and if these protons are not absorbed in the sources, but rather contribute to the UHECR flux observed, then the energy content in the neutrino flux can not be higher than the one in UHECRs, leading to the so called Waxman-Bahcall bound [36, 38]. If one of these assumptions does not apply, such as for acceleration sources that are opaque to nucleons or in the TD scenarios where X particle decays produce much fewer nucleons than  $\gamma$ -rays and neutrinos, the Waxman-Bahcall bound does not apply, but the neutrino flux is still constrained by the observed diffuse  $\gamma$ -ray flux in the GeV range. This is true as long as the energy fluences produced in  $\gamma$ -rays and neutrinos are comparable, which follows from isospin symmetry if neutrinos are produced by pion production, because  $\gamma$ -rays injected above the pair production threshold on the CMB will cascade down to the GeV regime (see Sect. 4.4).

## 2 Present and Future UHE CR and Neutrino Experiments

The CR primaries are shielded by the Earth's atmosphere and near the ground reveal their existence only by indirect effects such as ionization. Indeed, it was the height dependence of this latter effect which led to the discovery of CRs by Hess in 1912. Direct observation of CR primaries is only possible from space by flying detectors with balloons or spacecraft. Naturally, such detectors are very limited in size and because the differential CR spectrum is a steeply falling function of energy (see Fig. 1), direct observations run out of statistics typically around a few 100 TeV.

Above  $\sim 100$  TeV, the showers of secondary particles created in the interactions of the primary CR with the atmosphere are extensive enough to be detectable from the ground. In the most traditional technique, charged hadronic particles, as well as electrons and muons in these Extensive Air Showers (EAS) are recorded on the ground [39] with standard instruments such as water Cherenkov detectors used in the old Volcano Ranch [6] and Haverah Park [8] experiments, and scintillation detectors which are used now-a-days. Currently operating ground arrays for UHECR EAS are the Yakutsk experiment in Russia [11] and the Akeno Giant Air Shower Array (AGASA) near Tokyo, Japan, which is the largest one, covering an area of roughly  $100 \text{ km}^2$  with about 100 detectors mutually separated by about 1 km [13]. The Sydney University Giant Air Shower Recorder (SUGAR) [7] operated until 1979 and was the largest array in the Southern hemisphere. The ground array technique allows one to measure a lateral cross section of the shower profile. The energy of the shower-initiating primary particle is estimated by appropriately parametrizing it in terms of a measurable parameter; traditionally this parameter is taken to be the particle density at 600 m from the shower core, which is found to be quite insensitive to the primary composition and

the interaction model used to simulate air showers.

The detection of secondary photons from EAS represents a complementary technique. The experimentally most important light sources are the fluorescence of air nitrogen excited by the charged particles in the EAS and the Cherenkov radiation from the charged particles that travel faster than the speed of light in the atmospheric medium. The first source is practically isotropic whereas the second one produces light strongly concentrated on the surface of a cone around the propagation direction of the charged source. The fluorescence technique can be used equally well for both charged and neutral primaries and was first used by the Fly’s Eye detector [12] and will be part of several future projects on UHECRs (see below). The primary energy can be estimated from the total fluorescence yield. Information on the primary composition is contained in the column depth  $X_{\max}$  (measured in  $\text{g cm}^{-2}$ ) at which the shower reaches maximal particle density. The average of  $X_{\max}$  is related to the primary energy  $E$  by

$$\langle X_{\max} \rangle = X'_0 \ln \left( \frac{E}{E_0} \right). \quad (1)$$

Here,  $X'_0$  is called the elongation rate and  $E_0$  is a characteristic energy that depends on the primary composition. Therefore, if  $X_{\max}$  and  $X'_0$  are determined from the longitudinal shower profile measured by the fluorescence detector, then  $E_0$  and thus the composition, can be extracted after determining the energy  $E$  from the total fluorescence yield. Comparison of CR spectra measured with the ground array and the fluorescence technique indicate systematic errors in energy calibration that are generally smaller than  $\sim 40\%$ . For a more detailed discussion of experimental EAS analysis with the ground array and the fluorescence technique see, e.g., Refs. [40].

As an upscaled version of the old Fly’s Eye Cosmic Ray experiment, the High Resolution Fly’s Eye detector has started to take data at Utah, USA [42]. Taking into account a duty cycle of about 10% (a fluorescence detector requires clear, moonless nights), the effective aperture of this instrument will be  $\simeq 350(1000) \text{ km}^2 \text{ sr}$  at 10(100) EeV, on average about 6 times the Fly’s Eye aperture, with a threshold around  $10^{17} \text{ eV}$ . Another project utilizing the fluorescence technique is the Japanese Telescope Array [43] which is currently in the proposal stage. If approved, its effective aperture will be about 10 times that of Fly’s Eye above  $10^{17} \text{ eV}$ , and it would also be used as a Cherenkov detector for TeV  $\gamma$ -ray astrophysics. The largest project presently under construction is the Pierre Auger Giant Array Observatory [44] planned for two sites, one in Argentina and another in the USA for maximal sky coverage. Each site will have a  $3000 \text{ km}^2$  ground array. The southern site will have about 1600 particle detectors (separated by 1.5 km each) overlooked by four fluorescence detectors. The ground arrays will have a duty cycle of nearly 100%, leading to an effective aperture about 30 times as large as the AGASA array. The corresponding cosmic ray event rate above  $10^{20} \text{ eV}$  will be about 50 events per year. About 10% of the events will be detected by both the ground array and the fluorescence component and can be used for cross calibration and detailed EAS studies. The energy threshold will be around  $10^{18} \text{ eV}$ , with full sensitivity above  $10^{19} \text{ eV}$ .

Recently NASA initiated a concept study for detecting EAS from space [46, 47] by observing their fluorescence light from an Orbiting Wide-angle Light-collector (OWL). This would provide an increase by another factor  $\sim 50$  in aperture compared to the Pierre Auger Project, corresponding to an event rate of up to a few thousand events per year above  $10^{20} \text{ eV}$ .

Similar concepts such as the Extreme Universe Space Observatory (EUSO) [48] which is part of the AirWatch program [49] and of which a prototype may be tested on the International Space Station are also being discussed. It is possible that the OWL and AirWatch efforts will merge. The energy threshold of such instruments would be between  $10^{19}$  and  $10^{20}$  eV. This technique would be especially suitable for detection of very small event rates such as those caused by UHE neutrinos which would produce deeply penetrating EAS (see Sect. 3.2). For more details on these recent experimental considerations see Ref. [50].

High energy neutrino astronomy is aiming towards a kilometer scale neutrino observatory. The major technique is the optical detection of Cherenkov light emitted by muons created in charged current reactions of neutrinos with nucleons either in water or in ice. The largest pilot experiments representing these two detector media are the now defunct Deep Undersea Muon and Neutrino Detection (DUMAND) experiment [51] in the deep sea near Hawai and the Antarctic Muon And Neutrino Detector Array (AMANDA) experiment [52] in the South Pole ice. Another water based experiment is situated at Lake Baikal [53]. Next generation deep sea projects include the French Astronomy with a Neutrino Telescope and Abyss environmental REsearch (ANTARES) [54] and the underwater Neutrino Experiment SouthwesT Of GRreece (NESTOR) project in the Mediterranean [55], whereas ICECUBE [56] represents the planned kilometer scale version of the AMANDA detector. Also under consideration are neutrino detectors utilizing techniques to detect the radio pulse from the electromagnetic showers created by neutrino interactions in ice and other materials (see Ref. [57]). This technique could possibly be scaled up to an effective area of  $10^4$  km<sup>2</sup> and a prototype is represented by the Radio Ice Cherenkov Experiment (RICE) experiment at the South Pole [58]. The Goldstone radio telescope has already put an upper limit on UHE neutrino fluxes [60] from the non-observation of radio pulses from showers induced by neutrinos interacting in the moons rim [61]. The sensitivity of existing underwater acoustic arrays to neutrino induced showers is also being studied [62]. Furthermore, neutrinos can also initiate horizontal EAS which can be detected by giant ground arrays and fluorescence detectors such as the Pierre Auger Project [63]. It has also been shown that the sensitivity of such experiments to UHE neutrinos could be significantly enhanced by triggering on Earth-skimming showers, i.e. showers with zenith angles slightly larger than  $90^\circ$  [64, 65, 66], especially for  $\tau$ -neutrinos. Finally, as mentioned above, deeply penetrating EAS could be detected from space by instruments such as the proposed space based AirWatch type detectors [46, 47, 48, 49]. More details and references on neutrino astronomy detectors are contained in Refs. [32, 67], and some recent overviews on neutrino astronomy can be found in Ref. [33].

## 3 Neutrino Interactions and Propagation

### 3.1 Neutrino propagation

The propagation of UHE neutrinos is governed mainly by their interaction with the relic neutrino background (RNB). In this section we give a short overview over the relevant interactions within the general framework for particle propagation used in the present contribution.

The average squared CM energy for interaction of an UHE neutrino of energy  $E$  with a



relic neutrino of energy  $\varepsilon$  is given by

$$\langle s \rangle \simeq (45 \text{ GeV})^2 \left( \frac{\varepsilon}{10^{-3} \text{ eV}} \right) \left( \frac{E}{10^{15} \text{ GeV}} \right). \quad (2)$$

If the relic neutrino is relativistic, then  $\varepsilon \simeq 3T_\nu(1+\eta_b/4)$  in Eq. (2), where  $T_\nu \simeq 1.9(1+z) \text{ K} = 1.6 \times 10^{-4}(1+z) \text{ eV}$  is the temperature at redshift  $z$  and  $\eta_b \lesssim 50$  is the dimensionless chemical potential of relativistic relic neutrinos. For nonrelativistic relic neutrinos of mass  $m_\nu \lesssim 20 \text{ eV}$ ,  $\varepsilon \simeq \max[3T_\nu, m_\nu]$ . Note that Eq. (2) implies interaction energies that are typically smaller than electroweak energies even for UHE neutrinos, except for energies near the Grand Unification scale,  $E \gtrsim 10^{15} \text{ GeV}$ , or if  $m_\nu \gtrsim 1 \text{ eV}$ . In this energy range, the cross sections are given by the Standard Model of electroweak interactions which are well confirmed experimentally. Physics beyond the Standard Model is, therefore, not expected to play a significant role in UHE neutrino interactions with the low energy relic backgrounds.

The dominant interaction mode of UHE neutrinos with the RNB is the exchange of a  $W^\pm$  boson in the t-channel ( $\nu_i + \bar{\nu}_j \rightarrow l_i + \bar{l}_j$ ), or of a  $Z^0$  boson in either the s-channel ( $\nu_i + \bar{\nu}_j \rightarrow f\bar{f}$ ) or the t-channel ( $\nu_i + \bar{\nu}_j \rightarrow \nu_i + \bar{\nu}_j$ ) [68, 69, 70, 71]. Here,  $i, j$  stands for either the electron, muon, or tau flavor, where  $i \neq j$  for the first reaction,  $l$  denotes a charged lepton, and  $f$  any charged fermion. If the latter is a quark, it will, of course, subsequently fragment into hadrons. As an example, the differential cross section for s-channel production of  $Z^0$  is given by

$$\frac{d\sigma_{\nu_i + \bar{\nu}_j \rightarrow Z^0 \rightarrow f\bar{f}}}{d\mu} = \frac{G_F^2 s}{4\pi} \frac{M_Z^2}{(s - M_Z^2)^2 + M_Z^2 \Gamma_Z^2} \left[ g_L^2 (1 + \mu^*)^2 + g_R^2 (1 - \mu^*)^2 \right], \quad (3)$$

where  $G_F$  is the Fermi constant,  $M_Z$  and  $\Gamma_Z$  are mass and lifetime of the  $Z^0$ ,  $g_L$  and  $g_R$  are the usual dimensionless left- and right-handed coupling constants for  $f$ , and  $\mu^*$  is the cosine of the scattering angle in the CM system.

The t-channel processes have cross sections that rise linearly with  $s$  up to  $s \simeq M_W^2$ , with  $M_W$  the  $W^\pm$  mass, above which they are roughly constant with a value  $\sigma_t(s \gtrsim M_W) \sim G_F^2 M_W^2 \sim 10^{-34} \text{ cm}^2$ . Using Eq. (2) this yields the rough estimate

$$\begin{aligned} \sigma_t(E, \varepsilon) &\sim \min \left[ 10^{-34}, 10^{-44} \left( \frac{s}{\text{MeV}^2} \right) \right] \text{ cm}^2 \\ &\sim \min \left[ 10^{-34}, 3 \times 10^{-39} \left( \frac{\varepsilon}{10^{-3} \text{ eV}} \right) \left( \frac{E}{10^{20} \text{ eV}} \right) \right] \text{ cm}^2. \end{aligned} \quad (4)$$

In contrast, within the Standard Model the neutrino-nucleon cross section roughly behaves as

$$\sigma_{\nu N}(E) \sim 10^{-31} (E/10^{20} \text{ eV})^{0.4} \text{ cm}^2 \quad (5)$$

for  $E \gtrsim 10^{15} \text{ eV}$  (see Eq.(7) below). Interactions of UHE neutrinos with nucleons are, however, still negligible compared to interactions with the RNB because the RNB particle density is about ten orders of magnitude larger than the baryon density. The only exception could occur near Grand Unification scale energies and at high redshifts and/or if contributions to the neutrino-nucleon cross section from physics beyond the Standard Model dominate at these energies (see Sect. 3.3 below).

It has recently been pointed out [72] that above the threshold for  $W^\pm$  production the process  $\nu + \gamma \rightarrow lW^\pm$  becomes comparable to the  $\nu\nu$  processes discussed above. Fig. 3 compares the cross sections relevant for neutrino propagation at CM energies around the electroweak scale. Again, for UHE neutrino interactions with the RNB the relevant CM energies can only be reached if (a) the UHE neutrino energy is close to the Grand Unification scale, or (b) the RNB neutrinos have masses in the eV regime, or (c) at redshifts  $z \gtrsim 10^3$ . Even then the  $\nu\gamma$  process never dominates over the  $\nu\nu$  process.

At lower energies there is an additional  $\nu\gamma$  interaction that was recently discussed as potentially important besides the  $\nu\nu$  processes: Using an effective Lagrangian derived from the Standard Model, Ref. [73] obtained the result  $\sigma_{\gamma+\nu \rightarrow \gamma+\gamma+\nu}(s) \simeq 9 \times 10^{-56} (s/\text{MeV}^2)^5 \text{cm}^2$ , supposed to be valid at least up to  $s \lesssim 10 \text{MeV}^2$ . Above the electron pair production threshold the cross section has not been calculated because of its complexity but is likely to level off and eventually decrease. Nevertheless, if the  $s^5$  behavior holds up to  $s \simeq$  a few hundred  $\text{MeV}^2$ , comparison with Eq. (4) shows that the process  $\gamma + \nu \rightarrow \gamma + \gamma + \nu$  would start to dominate and influence neutrino propagation around  $E \sim 3 \times 10^{17} (\varepsilon/10^{-3} \text{eV}) \text{eV}$ , as was pointed out in Ref. [74].

For a given source distribution, the contribution of the “direct” neutrinos to the flux can be computed from ( $t_0$  is the age of the Universe)

$$j(E) \simeq \frac{3}{8\pi} t_0 \int_0^{z(E)} dz_i (1+z_i)^{-9/2} \Phi[(1+z_i)E, z_i], \quad (6)$$

up to the interaction redshift  $z(E)$ , i.e. the average redshift from which a neutrino of present day energy  $E$  could have propagated without interacting. This approximation neglects the secondary neutrinos and the decay products of the leptons created in the neutral current and charged current reactions of UHE neutrinos with the RNB discussed above. Similarly to the EM case, these secondary particles can lead to neutrino cascades developing over cosmological redshifts [70].

Approximate expressions for the interaction redshift for the processes discussed above have been given in Refs. [14, 75] for CM energies below the electroweak scale, assuming relativistic, nondegenerate relic neutrinos,  $m_\nu \lesssim T_\nu$ , and  $\eta_b \ll 1$ . Approaching the electroweak scale, a resonance occurs in the interaction cross section for s-channel  $Z^0$  exchange at the  $Z^0$  mass,  $s = M_Z^2 \simeq (91 \text{GeV})^2$ , see Eq. (3). The absorption redshift for the corresponding neutrino energy,  $E \simeq 10^{15} \text{GeV} (\varepsilon/10^{-3} \text{eV})^{-1}$  drops to a few (or less for a degenerate, relativistic RNB) and asymptotically approaches constant values of a few tens at higher energies.

An interesting situation arises if the RNB consists of massive neutrinos with  $m_\nu \sim 1 \text{eV}$ : Such neutrinos would constitute hot dark matter which is expected to cluster [76], for example, in galaxy clusters. This would potentially increase the interaction probability for any neutrino of energy within the width of the  $Z^0$  resonance at  $E = M_Z^2/2m_\nu = 4 \times 10^{21} (\text{eV}/m_\nu) \text{eV}$ . Recently it has been suggested that the stable end products of the “Z-bursts” that would thus be induced at close-by distances ( $\lesssim 50 \text{Mpc}$ ) from Earth may explain the highest energy cosmic rays [77, 78] and may also provide indirect evidence for neutrino hot dark matter. These end products would be mostly nucleons and  $\gamma$ -rays with average energies a factor of  $\simeq 5$  and  $\simeq 40$  lower, respectively, than the original UHE neutrino. As a consequence, if the UHE neutrino was produced as a secondary of an accelerated proton, the

energy of the latter would have to be at least a few  $10^{22}$  eV [77], making Z-bursts above GZK energies more likely to play a role in the context of non-acceleration scenarios. Moreover, it has subsequently been pointed out [79] that Z production is dominated by annihilation on the non-clustered massive RNB compared to annihilation with neutrinos clustering in the Galactic halo or in nearby galaxy clusters. As a consequence, for a significant contribution of neutrino annihilation to the observed EHECR flux, a new class of neutrino sources, unrelated to UHECR sources, seems necessary. This has been confirmed by more detailed numerical simulations [80] where it has, however, also been demonstrated that the most significant contribution could come from annihilation on neutrino dark matter clustering in the Local Supercluster by amounts consistent with expectations. In the absence of any assumptions on the neutrino sources, the minimal constraint comes from the unavoidable production of secondary  $\gamma$ -rays contributing to the diffuse flux around 10 GeV measured by EGRET: If the Z-burst decay products are to explain EHECR, the massive neutrino overdensity  $f_\nu$  over a length scale  $l_\nu$  has to satisfy  $f_\nu \gtrsim 20 (l_\nu/5 \text{ Mpc})^{-1}$ , provided that only neutrinos leave the source, a situation that may arise in top-down models if the X particles decay exclusively into neutrinos (see Fig. 8 below for a model involving topological defects and Ref. [81] for a scenario involving decaying superheavy relic particles). If, instead, the total photon source luminosity is comparable to the total neutrino luminosity, as in most models, the EGRET constraint translates into the more stringent requirement  $f_\nu \gtrsim 10^3 (l_\nu/5 \text{ Mpc})^{-1}$ . This bound can only be relaxed if most of the EM energy is radiated in the TeV range where the Universe is more transparent [80]. Fig. 4 shows an example of this situation.

Furthermore, the Z-burst scenario requires sources that are optically thick for accelerated protons with respect to photo-pion production because otherwise the observable proton flux below the GZK cutoff would be comparable to the neutrino flux [89, 79]. A systematic parameter study of the required overdensity, based on analytical flux estimates, has been performed in Ref. [90]. Recently it has been noted that a degenerate relic neutrino background would increase the interaction probability and thereby make the Z-burst scenario more promising [91]. A neutrino asymmetry of order unity is not excluded phenomenologically [92] and can be created in the early Universe, for example, through the Affleck-Dine baryogenesis mechanism [93] or due to neutrino oscillations. The authors of Ref. [91] pointed out that for a neutrino mass  $m_\nu \simeq 0.07$  eV, a value suggested by the Super-Kamiokande experiment [3], and for sources at redshifts of a few, the flux of secondary Z-decay products is maximal for a RNB density parameter  $\Omega_\nu \simeq 0.01$ . Such neutrino masses, however, require the sources to produce neutrinos at least up to  $10^{22}$  eV.

UHE neutrinos from the decay of pions, that are produced by interactions of accelerated protons in astrophysical sources, must have originated within redshifts of a few. Moreover, in most conventional models their flux is expected to fall off rapidly above  $10^{20}$  eV. Examples are production in active galactic nuclei within hadronic models [94, 95, 96, 97, 98, 99], and “cosmogenic” neutrinos from interactions of UHECR nucleons (near or above the GZK cutoff) with the CMB (see, e.g., Refs. [100, 101]). The latter source is the only one that is guaranteed to exist due to existence of UHECRs near the GZK cutoff, but the fluxes are generally quite small. Therefore, interaction of these UHE neutrinos with the RNB, that could reveal the latter’s existence, can, if at all, be important only if the relic neutrinos have a mass  $m_\nu \gtrsim 1$  eV [68]. Due to the continuous release of UHE neutrinos up to much higher

redshifts, most top-down scenarios would imply substantially higher fluxes that also extend to much higher energies [75] (see Sect. 4.4 below). Certain features in the UHE neutrino spectrum predicted within such top-down scenarios, such as a change of slope for massless neutrinos [70] or a dip structure for relic neutrino masses of order 1 eV [71, 78], have therefore been proposed as possibly the only way to detect the RNB. However, some of the scenarios at the high end of neutrino flux predictions have recently been ruled out based on constraints on the accompanying energy release into the EM channel.

The recent claim that the Z-burst mechanism can explain the EHECR flux even without overdensity,  $f_\nu = 1$ , and even allows to determine the neutrino mass  $m_\nu \sim 1$  eV [102] was based on assumptions that we characterized here as highly unrealistic: Sources accelerating nuclei to  $\gtrsim 10^{23}$  eV while being completely opaque to both the primaries and the secondary photons. The energy fluence of the latter, however, after possibly being reprocessed to lower energies by EM cascading, must be comparable to the neutrino energy fluence by simple isospin symmetry in the production of charged and neutral pions.

Since in virtually all models UHE neutrinos are created as secondaries from pion decay, i.e. as electron or muon neutrinos,  $\tau$ -neutrinos can only be produced by a flavor changing  $W^\pm$  t-channel interaction with the RNB. The flux of UHE  $\tau$ -neutrinos is therefore usually expected to be substantially smaller than the one of electron and muon neutrinos, if no neutrino oscillations take place at these energies. However, the recent evidence from the Superkamiokande experiment for nearly maximal mixing between muon and  $\tau$ -neutrinos with  $|\Delta m^2| = |m_{\nu_\mu}^2 - m_{\nu_\tau}^2| \simeq 5 \times 10^{-3} \text{ eV}^2$  [3] would imply an oscillation length of  $L_{osc} = 2E/|\Delta m^2| = 2.6 \times 10^{-6} (E/\text{PeV})(|\Delta m^2|/5 \times 10^{-3} \text{ eV}^2)^{-1} \text{ pc}$  and, therefore, a rough equilibration between muon and  $\tau$ -neutrino fluxes from any source at a distance larger than  $L_{osc}$  [104]. Turning this around, one sees that a source at distance  $d$  emitting neutrinos of energy  $E$  is sensitive to neutrino mixing with  $|\Delta m^2| = 2E/d \simeq 1.3 \times 10^{-16} (E/\text{PeV})(d/100 \text{ Mpc})^{-1} \text{ eV}^2$  [105, 106]. Under certain circumstances, resonant conversion in the potential provided by the RNB clustering in galactic halos may also influence the flavor composition of UHE neutrinos from extraterrestrial sources [107]. In addition, such huge cosmological baselines can be sensitive probes of neutrino decay [108].

## 3.2 Neutrino detection

We now turn to a discussion of UHE neutrino interactions with matter relevant for neutrino detection. UHE neutrinos can be detected by detecting the muons produced in ordinary matter via charged-current reactions with nucleons; see, e.g., Refs. [109, 110, 111] for recent discussions. Corresponding cross sections are calculated by folding the fundamental standard model quark-neutrino cross section with the distribution function of the partons in the nucleon. These cross sections are most sensitive to the abundance of partons of fractional momentum  $x \simeq M_W^2/2m_N E$ , where  $E$  is the neutrino energy. For the relevant squared momentum transfer,  $Q^2 \sim M_W^2$ , these parton distribution functions have been measured down to  $x \simeq 0.02$  [112]. (It has been suggested that observation of the atmospheric neutrino flux with future neutrino telescopes may probe parton distribution functions at much smaller  $x$  currently inaccessible to colliders [113]). Currently, therefore, neutrino-nucleon cross sections for  $E \gtrsim 10^{14}$  eV can be obtained only by extrapolating the parton distribution functions to

lower  $x$ . Above  $10^{19}$  eV, the resulting uncertainty has been estimated to be a factor 2 [110], whereas within the dynamical radiative parton model it has been claimed to be at most 20 % [111]. An intermediate estimate using the CTEQ4-DIS distributions can roughly be parameterized by [110]

$$\sigma_{\nu N}(E) \simeq 2.36 \times 10^{-32} (E/10^{19} \text{ eV})^{0.363} \text{ cm}^2 \quad (10^{16} \text{ eV} \lesssim E \lesssim 10^{21} \text{ eV}). \quad (7)$$

Improved calculations including non-leading logarithmic contributions in  $1/x$  have recently been performed in Ref. [114]. The results for the neutrino-nucleon cross section differ by less than a factor 1.5 with Refs. [110, 111] even at  $10^{21}$  eV.

However, more recently it has been argued that the neutrino-nucleon cross-section calculated within the Standard Model becomes unreliable for  $E \gtrsim 2 \times 10^{17}$  eV: the authors of [115] used the  $O(g^2)$  expression for the elastic forward scattering amplitude to derive via the optical theorem the bound  $\sigma_{\nu N} \leq 9.3 \times 10^{-33} \text{ cm}^2$  for the total cross-section. Current parton distribution functions (pdf's) predict a violation of this unitarity bound above  $E \gtrsim 2 \times 10^{17}$  eV. The authors of [115] argue that the large  $O(g^4)$  corrections to the forward scattering amplitude necessary to restore unitarity signal a breakdown of electroweak perturbation theory. Alternatively, large changes in the evolution of the parton distribution functions have to set in soon after the kinematical range probed by HERA. A large  $O(g^4)$  correction to the forward scattering amplitude is, however, not surprising because the  $O(g^2)$  amplitude contains no resonant contribution and is real. In particular, the total cross-section is therefore not only bounded by a constant but zero at  $O(g^2)$ , and the imaginary part of the box diagram of  $O(g^4)$  is the *first* contribution to the total neutrino-nucleon cross-section [116].

Interestingly, it has been shown that the increasing target mass provided by the Earth for increasing zenith angles below the horizontal implies that the rate of up-going air showers in UHECR detectors does not decrease with decreasing neutrino-nucleon cross section but may even increase [66]. Thus, cross sections smaller than Eq. (7) do not lead to reduced event rates in UHECR detectors and can be measured from the angular distribution of events. UHECR and neutrino experiments can thus contribute to measure cross sections at energies inaccessible in accelerator experiments!

Neutral-current neutrino-nucleon cross sections are expected to be a factor 2-3 smaller than charged-current cross sections at UHE and interactions with electrons only play a role at the Glashow resonance,  $\bar{\nu}_e e \rightarrow W$ , at  $E = 6.3 \times 10^{15}$  eV. Furthermore, cross sections of neutrinos and anti-neutrinos are basically identical at UHE. Radiative corrections influence the total cross section negligibly compared to the parton distribution uncertainties, but may lead to an increase of the average inelasticity in the outgoing lepton from  $\simeq 0.19$  to  $\simeq 0.24$  at  $E \sim 10^{20}$  eV [117], although this would probably hardly influence the shower character.

Neutrinos propagating through the Earth start to be attenuated above  $\simeq 100$  TeV due to the increasing Standard Model cross section as indicated by Eq. (7). Detailed integrations of the relevant transport equations for muon neutrinos above a TeV have been presented in Ref. [114], and, for a general cold medium, in Ref. [118]. In contrast,  $\tau$ -neutrinos with energy up to  $\simeq 100$  PeV can penetrate the Earth due to their regeneration from  $\tau$  decays [106]. As a result, a primary UHE  $\tau$ -neutrino beam propagating through the Earth would cascade down below  $\simeq 100$  TeV and in a neutrino telescope could give rise to a higher total rate of upgoing events as compared to downgoing events for the same beam arriving from

above the horizon. As mentioned above, a primary  $\tau$ -neutrino beam could arise even in scenarios based on pion decay, if  $\nu_\mu - \nu_\tau$  mixing occurs with the parameters suggested by the Super-Kamiokande results [104]. In the PeV range,  $\tau$ -neutrinos can produce characteristic "double-bang" events where the first bang would be due to the charged-current production by the  $\tau$ -neutrino of a  $\tau$  whose decay at a typical distance  $\simeq 100$  m would produce the second bang [105]. These effects have also been suggested as an independent astrophysical test of the neutrino oscillation hypothesis. In addition, isotropic neutrino fluxes in the energy range between 10 TeV and 10 PeV have been suggested as probes of the Earth's density profile, whereby neutrino telescopes could be used for neutrino absorption tomography [119].

### 3.3 New Interactions

It has been suggested that the neutrino-nucleon cross section,  $\sigma_{\nu N}$ , can be enhanced by new physics beyond the electroweak scale in the center of mass (CM) frame, or above about a PeV in the nucleon rest frame [120, 121, 122]. Neutrino induced air showers may therefore rather directly probe new physics beyond the electroweak scale.

The lowest partial wave contribution to the cross section of a point-like particle is constrained by unitarity to be not much larger than a typical electroweak cross section [123]. However, at least two major possibilities allowing considerably larger cross sections have been discussed in the literature for which unitarity bounds need not be violated. In the first, a broken SU(3) gauge symmetry dual to the unbroken SU(3) color gauge group of strong interaction is introduced as the "generation symmetry" such that the three generations of leptons and quarks represent the quantum numbers of this generation symmetry. In this scheme, neutrinos can have close to strong interaction cross sections with quarks. In addition, neutrinos can interact coherently with all partons in the nucleon, resulting in an effective cross section comparable to the geometrical nucleon cross section. This model lends itself to experimental verification through shower development altitude statistics [120].

The second possibility consists of a large increase in the number of degrees of freedom above the electroweak scale [124]. A specific implementation of this idea is given in theories with  $n$  additional large compact dimensions and a quantum gravity scale  $M_{4+n} \sim \text{TeV}$  that has recently received much attention in the literature [125] because it provides an alternative solution (i.e., without supersymmetry) to the hierarchy problem in grand unifications of gauge interactions. The cross sections within such scenarios have not been calculated from first principles yet. Within the field theory approximation which should hold for squared CM energies  $s \lesssim M_{4+n}^2$ , the spin 2 character of the graviton predicts  $\sigma_g \sim s^2/M_{4+n}^6$  [126]. For  $s \gg M_{4+n}^2$ , several arguments based on unitarity within field theory have been put forward. The emission of massive Kaluza-Klein (KK) graviton modes associated with the increased phase space due to the extra dimensions leads to the rough estimate (derived for  $n = 2$ ) [126]

$$\sigma_g \simeq \frac{4\pi s}{M_{4+n}^4} \simeq 10^{-27} \left( \frac{M_{4+n}}{\text{TeV}} \right)^{-4} \left( \frac{E}{10^{20} \text{ eV}} \right) \text{ cm}^2, \quad (8)$$

where in the last expression we specified to a neutrino of energy  $E$  hitting a nucleon at rest. A more detailed calculation taking into account scattering on individual partons leads to similar orders of magnitude [122]. Note that a neutrino would typically start to interact in

the atmosphere for  $\sigma_{\nu N} \gtrsim 10^{-27} \text{ cm}^2$ , i.e. in the case of Eq. (8) for  $E \gtrsim 10^{20} \text{ eV}$ , assuming  $M_{4+n} \simeq 1 \text{ TeV}$ . For cross sections such large the neutrino therefore becomes a primary candidate for the observed EHECR events. However, since in a neutral current interaction the neutrino transfers only about 10% of its energy to the shower, the cross section probably has to be at least a few  $10^{-26} \text{ cm}^2$  to be consistent with observed showers which start within the first  $50 \text{ g cm}^{-2}$  of the atmosphere [127, 128]. A specific signature of this scenario would be the absence of any events above the energy where  $\sigma_g$  grows beyond  $\simeq 10^{-27} \text{ cm}^2$  in neutrino telescopes based on ice or water as detector medium [129], and a hardening of the spectrum above this energy in atmospheric detectors such as the Pierre Auger Project [44] and the proposed space based AirWatch type detectors [46, 48, 49]. Furthermore, according to Eq. (8), the average atmospheric column depth of the first interaction point of neutrino induced EAS in this scenario is predicted to depend linearly on energy. This should be easy to distinguish from the logarithmic scaling expected for nucleons, nuclei, and  $\gamma$ -rays. To test such scalings one can, for example, take advantage of the fact that the atmosphere provides a detector medium whose column depth increases from  $\sim 1000 \text{ g/cm}^2$  towards the zenith to  $\sim 36000 \text{ g/cm}^2$  towards horizontal arrival directions. This probes cross sections in the range  $\sim 10^{-29} - 10^{-27} \text{ cm}^2$ . Due to the increased column depth, water/ice detectors would probe cross sections in the range  $\sim 10^{-31} - 10^{-29} \text{ cm}^2$  [130] which could be relevant for TeV scale gravity models [131].

From a perturbative point of view within string theory,  $\sigma_{\nu N}$  can be estimated as follows: Individual amplitudes are expected to be suppressed exponentially above the string scale  $M_s$  which again for simplicity we assume here to be comparable to  $M_{4+n}$ . This can be interpreted as a result of the finite spatial extension of the string states. In this case, the neutrino nucleon cross section would be dominated by interactions with the partons carrying a momentum fraction  $x \sim M_s^2/s$ , leading to [127]

$$\begin{aligned} \sigma_{\nu N} &\simeq \frac{4\pi}{M_s^2} \ln(s/M_s^2) (s/M_s^2)^{0.363} \simeq 6 \times 10^{-29} \left( \frac{M_s}{\text{TeV}} \right)^{-4.726} \left( \frac{E}{10^{20} \text{ eV}} \right)^{0.363} \\ &\times \left[ 1 + 0.08 \ln \left( \frac{E}{10^{20} \text{ eV}} \right) - 0.16 \ln \left( \frac{M_s}{\text{TeV}} \right) \right]^2 \text{ cm}^2 \end{aligned} \quad (9)$$

This is probably too small to make neutrinos primary candidates for the highest energy showers observed, given the fact that complementary constraints from accelerator experiments result in  $M_s \gtrsim 1 \text{ TeV}$  [132]. On the other hand, general arguments on the production of “string balls” or small black holes from two point particles represented by light strings [133] leads to the asymptotic scaling  $\sigma \simeq (s/M_s^2)^{1/(n+1)}$  for  $s \gtrsim M_s^2$  for the fundamental neutrino-parton cross section. This could lead to values for  $\sigma_{\nu N}$  larger than Eq. (9) [134]. Some other recent work seems to imply that in TeV string models cross sections, if not sufficient to make neutrinos UHECR primary candidates, could at least be significantly larger than Standard Model cross sections [135]. Thus, an experimental detection of the signatures discussed in this section could lead to constraints on some string-inspired models of extra dimensions.

There are, however, severe astrophysical and cosmological constraints on  $M_{4+n}$  which result from limiting the emission of bulk gravitons into the extra dimensions. The strongest constraints in this regard come from the production due to nucleon-nucleon bremsstrahlung in type II supernovae [136] and their subsequent decay into a diffuse background of  $\gamma$ -rays in

the MeV range [137]. The latter read  $M_6 \gtrsim 84 \text{ TeV}$ ,  $M_7 \gtrsim 7 \text{ TeV}$ , for  $n = 2, 3$ , respectively, and, therefore,  $n \geq 5$  is required if neutrino primaries are to serve as a primary candidate for the EHECR events observed above  $10^{20} \text{ eV}$ . This assumes a toroidal geometry of the extra dimensions with equal radii given by

$$r_n \simeq M_{4+n}^{-1} \left( \frac{M_{\text{Pl}}}{M_{4+n}} \right)^{2/n} \simeq 2 \times 10^{-17} \left( \frac{\text{TeV}}{M_{4+n}} \right) \left( \frac{M_{\text{Pl}}}{M_{4+n}} \right)^{2/n} \text{ cm}, \quad (10)$$

where  $M_{\text{Pl}}$  denotes the Planck mass. The above lower bounds on  $M_{4+n}$  thus translate into the corresponding upper bounds  $r_2 \lesssim 0.9 \times 10^{-4} \text{ mm}$ ,  $r_3 \lesssim 0.19 \times 10^{-6} \text{ mm}$ , respectively. Still stronger but somewhat more model dependent bounds result from the production of KK modes during the reheating phase after inflation. For example, a bound  $M_6 \gtrsim 500 \text{ TeV}$  has been reported [138] based on the contribution to the diffuse  $\gamma$ -ray background in the 100 MeV region. We note, however, that all astrophysical and cosmological bounds are changed in more complicated geometries of extra dimensions [139].

The neutrino primary hypothesis of EHECR together with other astrophysical and cosmological constraints thus provides an interesting testing ground for theories involving large compact extra dimensions representing one possible kind of physics beyond the Standard Model. In this context, we mention that in theories with large compact extra dimensions mentioned above, Newton's law of gravity is expected to be modified at distances smaller than the length scale given by Eq. (10). Indeed, there are laboratory experiments measuring gravitational interaction at small distances (for a recent review of such experiments see Ref. [140]), which also probe these theories. Thus, future EHECR experiments and gravitational experiments in the laboratory together have the potential of providing rather strong tests of these theories. These tests would be complementary to constraints from collider experiments [132].

Independent of theoretical arguments, the EHECR data can be used to put constraints on cross sections satisfying  $\sigma_{\nu N}(E \gtrsim 10^{19} \text{ eV}) \lesssim 10^{-27} \text{ cm}^2$ . Particles with such cross sections would give rise to horizontal air showers. The Fly's Eye experiment established an upper limit on horizontal air showers [88]. The non-observation of the neutrino flux expected from pions produced by EHECRs interacting with the CMB the results in the limit [141, 130]

$$\begin{aligned} \sigma_{\nu N}(10^{17} \text{ eV}) &\lesssim 1 \times 10^{-29} / \bar{y}^{1/2} \text{ cm}^2 \\ \sigma_{\nu N}(10^{18} \text{ eV}) &\lesssim 8 \times 10^{-30} / \bar{y}^{1/2} \text{ cm}^2 \\ \sigma_{\nu N}(10^{19} \text{ eV}) &\lesssim 5 \times 10^{-29} / \bar{y}^{1/2} \text{ cm}^2, \end{aligned} \quad (11)$$

where  $\bar{y}$  is the average energy fraction of the neutrino deposited into the shower ( $\bar{y} = 1$  for charged current reactions and  $\bar{y} \simeq 0.1$  for neutral current reactions). Neutrino fluxes predicted in various scenarios are shown in Fig. 5. The projected sensitivity of future experiments such as the Pierre Auger Observatories and the AirWatch type satellite projects indicate that the cross section limits Eq. (11) could be improved by up to four orders of magnitude, corresponding to one order of magnitude in  $M_s$  or  $M_{4+n}$ . This would close the window between cross sections allowing horizontal air showers,  $\sigma_{\nu N}(E \gtrsim 10^{19} \text{ eV}) \lesssim 10^{-27} \text{ cm}^2$ , and the Standard Model value Eq. (7).



We note in this context that, only assuming  $3+1$  dimensional field theory, consistency of the UHE  $\nu N$  cross section with data at electroweak energies does not lead to very stringent constraints: Relating the cross section to the  $\nu N$  elastic amplitude in a model independent way yields [145]

$$\sigma(E) \lesssim 3 \times 10^{-24} \left( \frac{E}{10^{19} \text{ eV}} \right) \text{ cm}^2. \quad (12)$$

However, it has been argued [115] (see discussion above), cross sections  $\sigma_{\nu N} \gtrsim 9.3 \times 10^{-33} \text{ cm}^2$  could signal a breakdown of perturbation theory.

In the context of conventional astrophysical sources, the relevant UHE neutrino primaries could, of course, only be produced as secondaries in interactions with matter or with low energy photons of protons or nuclei accelerated to energies of at least  $10^{21}$  eV. This implies strong requirements on the possible sources.

In addition, neutrino primaries with new interactions would predict a significant correlation of UHECR arrival directions with high redshift objects. Indeed, various claims recently occurred in the literature for significant angular correlations of UHECRs with certain astrophysical objects at distances too large for the primaries to be nucleons, nuclei, or  $\gamma$ -rays. Farrar and Biermann reported a possible correlation between the arrival direction of the five highest energy CR events and compact radio quasars at redshifts between 0.3 and 2.2 [146] Undoubtedly, with the present amount of data the interpretation of such evidence for a correlation remains somewhat subjective, as is demonstrated by the criticism of the statistical analysis in Ref. [146] by Hoffman [147] and the reply by Farrar and Biermann [148]). Also, a new analysis with the somewhat larger data set now available did not support such correlations [149]. This is currently disputed since another group claims to have found a correlation on the 99.9% confidence level [150]. Most recently, a correlation between UHECRs of energy  $E \gtrsim 4 \times 10^{19}$  eV and BL Lacertae objects at redshifts  $z > 0.1$  was claimed [151]. None of these claims are convincing yet but confirmation or refutation should be possible within the next few years by the new experiments. Clearly, a confirmation of one of these correlations would be exciting as it would probably imply new physics such as neutrinos with new interactions, as yet unknown, e.g. supersymmetric, particles, or even more radical propositions such as violation of Lorentz invariance (for a discussion of these latter possibilities see, e.g., Refs. [19]).

## 4 Top-Down Scenarios

### 4.1 The Main Idea

As mentioned in the introduction, all top-down scenarios involve the decay of X particles of mass close to the GUT scale which can basically be produced in two ways: If they are very short lived, as usually expected in many GUTs, they have to be produced continuously. The only way this can be achieved is by emission from topological defects left over from cosmological phase transitions that may have occurred in the early Universe at temperatures close to the GUT scale, possibly during reheating after inflation. Topological defects necessarily occur between regions that are causally disconnected, such that the orientation of the order parameter associated with the phase transition can not be communicated between these

regions and consequently will adopt different values. Examples are cosmic strings (similar to vortices in superfluid helium), magnetic monopoles, and domain walls (similar to Bloch walls separating regions of different magnetization in a ferromagnet). The defect density is consequently given by the particle horizon in the early Universe and their formation can even be studied in solid state experiments where the expansion rate of the Universe corresponds to the quenching speed with which the phase transition is induced [152]. The defects are topologically stable, but in the cosmological case time dependent motion leads to the emission of particles with a mass comparable to the temperature at which the phase transition took place. The associated phase transition can also occur during reheating after inflation.

Alternatively, instead of being released from topological defects, X particles may have been produced directly in the early Universe and, due to some unknown symmetries, have a very long lifetime comparable to the age of the Universe. In contrast to Weakly-Interacting Massive Particles (WIMPS) below a few hundred TeV which are the usual dark matter candidates motivated by, for example, supersymmetry and can be produced by thermal freeze out, such superheavy X particles have to be produced non-thermally. Several such mechanisms operating in the post-inflationary epoch in the early Universe have been studied. They include gravitational production through the effect of the expansion of the background metric on the vacuum quantum fluctuations of the X particle field, or creation during reheating at the end of inflation if the X particle field couples to the inflaton field. The latter case can be divided into three subcases, namely “incoherent” production with an abundance proportional to the X particle annihilation cross section, non-adiabatic production in broad parametric resonances with the oscillating inflaton field during preheating (analogous to energy transfer in a system of coupled pendula), and creation in bubble wall collisions if inflation is completed by a first order phase transition. In all these cases, such particles, also called “WIMPZILLAs”, would contribute to the dark matter and their decays could still contribute to UHE CR fluxes today, with an anisotropy pattern that reflects the dark matter distribution in the halo of our Galaxy.

It is interesting to note that one of the prime motivations of the inflationary paradigm was to dilute excessive production of “dangerous relics” such as topological defects and superheavy stable particles. However, such objects can be produced right after inflation during reheating in cosmologically interesting abundances, and with a mass scale roughly given by the inflationary scale which in turn is fixed by the CMB anisotropies to  $\sim 10^{13}$  GeV [153]. The reader will realize that this mass scale is somewhat above the highest energies observed in CRs, which implies that the decay products of these primordial relics could well have something to do with EHECRs which in turn can probe such scenarios!

For dimensional reasons the spatially averaged X particle injection rate can only depend on the mass scale  $m_X$  and on cosmic time  $t$  in the combination

$$\dot{n}_X(t) = \kappa m_X^p t^{-4+p}, \quad (13)$$

where  $\kappa$  and  $p$  are dimensionless constants whose value depend on the specific top-down scenario [75], For example, the case  $p = 1$  is representative of scenarios involving release of X particles from topological defects, such as ordinary cosmic strings [154], necklaces [155] and magnetic monopoles [156]. This can be easily seen as follows: The energy density  $\rho_s$  in a network of defects has to scale roughly as the critical density,  $\rho_s \propto \rho_{\text{crit}} \propto t^{-2}$ , where

$t$  is cosmic time, otherwise the defects would either start to overclose the Universe, or end up having a negligible contribution to the total energy density. In order to maintain this scaling, the defect network has to release energy with a rate given by  $\dot{\rho}_s = -a\rho_s/t \propto t^{-3}$ , where  $a = 1$  in the radiation dominated era, and  $a = 2/3$  during matter domination. If most of this energy goes into emission of X particles, then typically  $\kappa \sim \mathcal{O}(1)$ . In the flux calculations for TD models presented in this paper, it was assumed that the X particles are nonrelativistic at decay.

The X particles could be gauge bosons, Higgs bosons, superheavy fermions, etc. depending on the specific GUT. They would have a mass  $m_X$  comparable to the symmetry breaking scale and would decay into leptons and/or quarks of roughly comparable energy. The quarks interact strongly and hadronize into nucleons ( $N$ s) and pions, the latter decaying in turn into  $\gamma$ -rays, electrons, and neutrinos. Given the X particle production rate,  $dn_X/dt$ , the effective injection spectrum of particle species  $a$  ( $a = \gamma, N, e^\pm, \nu$ ) via the hadronic channel can be written as  $(dn_X/dt)(2/m_X)(dN_a/dx)$ , where  $x \equiv 2E/m_X$ , and  $dN_a/dx$  is the relevant fragmentation function (FF).

We adopt the Local Parton Hadron Duality (LPHD) approximation [157] according to which the total hadronic FF,  $dN_h/dx$ , is taken to be proportional to the spectrum of the partons (quarks/gluons) in the parton cascade (which is initiated by the quark through perturbative QCD processes) after evolving the parton cascade to a stage where the typical transverse momentum transfer in the QCD cascading processes has come down to  $\sim R^{-1} \sim$  few hundred MeV, where  $R$  is a typical hadron size. The parton spectrum is obtained from solutions of the standard QCD evolution equations in modified leading logarithmic approximation (MLLA) which provides good fits to accelerator data at LEP energies [157]. We will specifically use a recently suggested generalization of the MLLA spectrum that includes the effects of supersymmetry [158]. Within the LPHD hypothesis, the pions and nucleons after hadronization have essentially the same spectrum. The LPHD does not, however, fix the relative abundance of pions and nucleons after hadronization. Motivated by accelerator data, we assume the nucleon content  $f_N$  of the hadrons to be in the range 3 to 10%, independent of energy, and the rest pions distributed equally among the three charge states. For  $x \lesssim 0.1$  this ratio as well as the spectra are roughly consistent with recent more detailed Monte Carlo simulations [159, 160]. This is also the range relevant for comparison with observations as long as  $m_X \gg 10^{12}$  GeV, which covers the range considered in the present paper. Resulting normalization ambiguities [159] are of factors of a few and thus subdominant in light of many other uncertainties at the current stage of these scenarios. The standard pion decay spectra then give the injection spectra of  $\gamma$ -rays, electrons, and neutrinos. For more details concerning uncertainties in the X particle decay spectra see Ref. [82].

## 4.2 Numerical Simulations

The  $\gamma$ -rays and electrons produced by X particle decay initiate electromagnetic (EM) cascades on low energy radiation fields such as the CMB. The high energy photons undergo electron-positron pair production (PP;  $\gamma\gamma_b \rightarrow e^-e^+$ ), and at energies below  $\sim 10^{14}$  eV they interact mainly with the universal infrared and optical (IR/O) backgrounds, while above

$\sim 100$  EeV they interact mainly with the universal radio background (URB). In the Klein-Nishina regime, where the CM energy is large compared to the electron mass, one of the outgoing particles usually carries most of the initial energy. This “leading” electron (positron) in turn can transfer almost all of its energy to a background photon via inverse Compton scattering (ICS;  $e\gamma_b \rightarrow e'\gamma$ ). EM cascades are driven by this cycle of PP and ICS. The energy degradation of the “leading” particle in this cycle is slow, whereas the total number of particles grows exponentially with time. This makes a standard Monte Carlo treatment difficult. Implicit numerical schemes have therefore been used to solve the relevant kinetic equations. A detailed account of the transport equation approach used in the calculations whose results are presented in this contribution can be found in Ref. [161]. All EM interactions that influence the  $\gamma$ -ray spectrum in the energy range  $10^8 \text{ eV} < E < 10^{25} \text{ eV}$ , namely PP, ICS, triplet pair production (TPP;  $e\gamma_b \rightarrow ee^-e^+$ ), and double pair production (DPP,  $\gamma\gamma_b \rightarrow e^-e^+e^-e^+$ ), as well as synchrotron losses of electrons in the large scale extragalactic magnetic field (EGMF), are included.

Similarly to photons, UHE neutrinos give rise to neutrino cascades in the primordial neutrino background via exchange of W and Z bosons [162, 71]. Besides the secondary neutrinos which drive the neutrino cascade, the W and Z decay products include charged leptons and quarks which in turn feed into the EM and hadronic channels. Neutrino interactions become especially significant if the relic neutrinos have masses  $m_\nu$  in the eV range and thus constitute hot dark matter, because the Z boson resonance then occurs at an UHE neutrino energy  $E_{\text{res}} = 4 \times 10^{21} (\text{eV}/m_\nu) \text{ eV}$ . In fact, this has been proposed as a significant source of EHECRs [78, 80]. Motivated by recent experimental evidence for neutrino mass we assume the neutrino masses to be  $m_{\nu_e} = 0.1 \text{ eV}$ ,  $m_{\nu_\mu} = m_{\nu_\tau} = 1 \text{ eV}$  and implemented the relevant W boson interactions in the t-channel and the Z boson exchange via t- and s-channel. Hot dark matter is also expected to cluster, potentially increasing secondary  $\gamma$ -ray and nucleon production [78, 80]. This influences mostly scenarios where X decays into neutrinos only. We parametrize massive neutrino clustering by a length scale  $l_\nu$  and an overdensity  $f_\nu$  over the average density  $\bar{n}_\nu$ . The Fermi distribution with a velocity dispersion  $v$  yields  $f_\nu \lesssim v^3 m_\nu^3 / (2\pi)^{3/2} / \bar{n}_\nu \simeq 330 (v/500 \text{ km sec}^{-1})^3 (m_\nu/\text{eV})^3$  [163]. Therefore, values of  $l_\nu \simeq$  few Mpc and  $f_\nu \simeq 20$  are conceivable on the local Supercluster scale [80].

The relevant nucleon interactions implemented are pair production by protons ( $p\gamma_b \rightarrow pe^-e^+$ ), photoproduction of single or multiple pions ( $N\gamma_b \rightarrow N n\pi$ ,  $n \geq 1$ ), and neutron decay. In TD scenarios, the particle injection spectrum is generally dominated by the “primary”  $\gamma$ -rays and neutrinos over nucleons. These primary  $\gamma$ -rays and neutrinos are produced by the decay of the primary pions resulting from the hadronization of quarks that come from the decay of the X particles. The contribution of secondary  $\gamma$ -rays, electrons, and neutrinos from decaying pions that are subsequently produced by the interactions of nucleons with the CMB, is in general negligible compared to that of the primary particles; we nevertheless include the contribution of the secondary particles in our code.

In principle, new interactions such as the ones involving a TeV quantum gravity scale can not only modify the interactions of primary particles in the detector, as discussed in Sect. 3.3, but also their propagation. However,  $\gamma$ -rays and nuclei interact mostly with the CMB and IR for which the CM energy is at most  $\simeq 30(E/10^{14} \text{ GeV})^{1/2} \text{ GeV}$ . At such energies the new interactions are much weaker than the dominating electromagnetic and

strong interactions. It has been suggested recently [164] that new interactions may notably influence UHE neutrino propagation. However, for neutrinos of mass  $m_\nu$ , the CM energy is  $\simeq 100(E/10^{14} \text{ GeV})^{1/2}(m_\nu/0.1 \text{ eV})^{1/2} \text{ GeV}$ , and therefore, UHE neutrino propagation would only be significantly modified for neutrino masses significantly larger than 0.1 eV. We will therefore ignore this possibility here.

We assume a flat Universe with no cosmological constant, and a Hubble constant of  $h = 0.65$  in units of  $100 \text{ km sec}^{-1}\text{Mpc}^{-1}$  throughout. The numerical calculations follow *all* produced particles in the EM, hadronic, and neutrino channel, whereas the often-used continuous energy loss (CEL) approximation (e.g., [165]) follows only the leading cascade particles. The CEL approximation can significantly underestimate the cascade flux at lower energies.

The two major uncertainties in the particle transport are the intensity and spectrum of the URB for which there exists only an estimate above a few MHz frequency [166], and the average value of the EGMF. To bracket these uncertainties, simulations have been performed for the observational URB estimate from Ref. [166] that has a low-frequency cutoff at 2 MHz (“minimal”), and the medium and maximal theoretical estimates from Ref. [83], as well as for EGMFs between zero and  $10^{-9} \text{ G}$ , the latter motivated by limits from Faraday rotation measurements [167]. A strong URB tends to suppress the UHE  $\gamma$ -ray flux by direct absorption whereas a strong EGMF blocks EM cascading (which otherwise develops efficiently especially in a low URB) by synchrotron cooling of the electrons. For the IR/O background we used the most recent data [168].

### 4.3 Results: $\gamma$ -ray and Nucleon Fluxes

Fig. 6 shows results from Ref. [82] for the time averaged  $\gamma$ -ray and nucleon fluxes in a typical TD scenario, assuming no EGMF, along with current observational constraints on the  $\gamma$ -ray flux. The spectrum was optimally normalized to allow for an explanation of the observed EHECR events, assuming their consistency with a nucleon or  $\gamma$ -ray primary. The flux below  $\lesssim 2 \times 10^{19} \text{ eV}$  is presumably due to conventional acceleration in astrophysical sources and was not fit. Similar spectral shapes have been obtained in Ref. [169], where the normalization was chosen to match the observed differential flux at  $3 \times 10^{20} \text{ eV}$ . This normalization, however, leads to an overproduction of the integral flux at higher energies, whereas above  $10^{20} \text{ eV}$ , the fits shown in Figs. 6 and 7 have likelihood significances above 50% (see Ref. [170] for details) and are consistent with the integral flux above  $3 \times 10^{20} \text{ eV}$  estimated in Refs. [12, 13]. The PP process on the CMB depletes the photon flux above 100 TeV, and the same process on the IR/O background causes depletion of the photon flux in the range 100 GeV–100 TeV, recycling the absorbed energies to energies below 100 GeV through EM cascading (see Fig. 6). The predicted background is *not* very sensitive to the specific IR/O background model, however [171]. The scenario in Fig. 6 obviously obeys all current constraints within the normalization ambiguities and is therefore quite viable. Note that the diffuse  $\gamma$ -ray background measured by EGRET [84] up to 10 GeV puts a strong constraint on these scenarios, especially if there is already a significant contribution to this background from conventional sources such as unresolved  $\gamma$ -ray blazars [172]. However, the  $\gamma$ -ray background constraint can be circumvented by assuming that TDs or the decaying

long lived X particles do not have a uniform density throughout the Universe but cluster within galaxies [173]. As can also be seen, at energies above 100 GeV, TD models are not significantly constrained by observed  $\gamma$ -ray fluxes yet (see Ref. [19] for more details on these measurements).

Fig. 7 shows results for the same TD scenario as in Fig. 6, but for a high EGMF  $\sim 10^{-9}$  G, somewhat below the current upper limit [167]. In this case, rapid synchrotron cooling of the initial cascade pairs quickly transfers energy out of the UHE range. The UHE  $\gamma$ -ray flux then depends mainly on the absorption length due to pair production and is typically much lower [165, 174]. (Note, though, that for  $m_X \gtrsim 10^{25}$  eV, the synchrotron radiation from these pairs can be above  $10^{20}$  eV, and the UHE flux is then not as low as one might expect.) We note, however, that the constraints from the EGRET measurements do not change significantly with the EGMF strength as long as the nucleon flux is comparable to the  $\gamma$ -ray flux at the highest energies, as is the case in Figs. 6 and 7. The results of Ref. [82] differ from those of Ref. [169] which obtained more stringent constraints on TD models because of the use of an older fragmentation function from Ref. [175], and a stronger dependence on the EGMF because of the use of a weaker EGMF which lead to a dominance of  $\gamma$ -rays above  $\simeq 10^{20}$  eV.

The energy loss and absorption lengths for UHE nucleons and photons are short ( $\lesssim 100$  Mpc). Thus, their predicted UHE fluxes are independent of cosmological evolution. The  $\gamma$ -ray flux below  $\simeq 10^{11}$  eV, however, scales as the total X particle energy release integrated over all redshifts and increases with decreasing  $p$  [176]. For  $m_X = 2 \times 10^{16}$  GeV, scenarios with  $p < 1$  are therefore ruled out (as can be inferred from Figs. 6 and 7), whereas constant comoving injection models ( $p = 2$ ) are well within the limits.

We now turn to signatures of TD models at UHE. The full cascade calculations predict  $\gamma$ -ray fluxes below 100 EeV that are a factor  $\simeq 3$  and  $\simeq 10$  higher than those obtained using the CEL or absorption approximation often used in the literature, in the case of strong and weak URB, respectively. Again, this shows the importance of non-leading particles in the development of unsaturated EM cascades at energies below  $\sim 10^{22}$  eV. Our numerical simulations give a  $\gamma$ /CR flux ratio at  $10^{19}$  eV of  $\simeq 0.1$ . The experimental exposure required to detect a  $\gamma$ -ray flux at that level is  $\simeq 4 \times 10^{19}$  cm<sup>2</sup> sec sr, about a factor 10 smaller than the current total experimental exposure. These exposures are well within reach of the Pierre Auger Cosmic Ray Observatories [44], which may be able to detect a neutral CR component down to a level of 1% of the total flux. In contrast, if the EGMF exceeds  $\sim 10^{-11}$  G, then UHE cascading is inhibited, resulting in a lower UHE  $\gamma$ -ray spectrum. In the  $10^{-9}$  G scenario of Fig. 7, the  $\gamma$ /CR flux ratio at  $10^{19}$  eV is 0.02, significantly lower than for no EGMF.

It is clear from the above discussions that the predicted particle fluxes in the TD scenario are currently uncertain to a large extent due to particle physics uncertainties (e.g., mass and decay modes of the X particles, the quark fragmentation function, the nucleon fraction  $f_N$ , and so on) as well as astrophysical uncertainties (e.g., strengths of the radio and infrared backgrounds, extragalactic magnetic fields, etc.). More details on the dependence of the predicted UHE particle spectra and composition on these particle physics and astrophysical uncertainties are contained in Ref. [82]. A detailed study of the uncertainties involved in the propagation of UHE nucleons,  $\gamma$ -rays, and neutrinos is currently underway [177].

We stress here that there are viable TD scenarios which predict nucleon fluxes that are comparable to or even higher than the  $\gamma$ -ray flux at all energies, even though  $\gamma$ -rays dominate at production. This occurs, e.g., in the case of high URB and/or for a strong EGMF, and a nucleon fragmentation fraction of  $\simeq 10\%$ ; see, for example, Fig. 7. Some of these TD scenarios would therefore remain viable even if EHECR induced EAS should be proven inconsistent with photon primaries (see, e.g., Ref. [178]). This is in contrast to scenarios with decaying massive dark matter in the Galactic halo which, due to the lack of absorption, predict compositions directly given by the fragmentation function, i.e. domination by  $\gamma$ -rays.

The normalization procedure to the EHECR flux described above imposes the constraint  $Q_{\text{EHECR}}^0 \lesssim 10^{-22} \text{ eV cm}^{-3} \text{ sec}^{-1}$  within a factor of a few [169, 82, 179] for the total energy release rate  $Q_0$  from TDs at the current epoch. In most TD models, because of the unknown values of the parameters involved, it is currently not possible to calculate the exact value of  $Q_0$  from first principles, although it has been shown that the required values of  $Q_0$  (in order to explain the EHECR flux) mentioned above are quite possible for certain kinds of TDs. Some cosmic string simulations and the necklace scenario suggest that defects may lose most of their energy in the form of X particles and estimates of this rate have been given [180, 155]. If that is the case, the constraint on  $Q_{\text{EHECR}}^0$  translates via Eq. (13) into a limit on the symmetry breaking scale  $\eta$  and hence on the mass  $m_X$  of the X particle:  $\eta \sim m_X \lesssim 10^{13} \text{ GeV}$  [181]. Independently of whether or not this scenario explains EHECR, the EGRET measurement of the diffuse GeV  $\gamma$ -ray background leads to a similar bound,  $Q_{\text{EM}}^0 \lesssim 2.2 \times 10^{-23} h(3p-1) \text{ eV cm}^{-3} \text{ sec}^{-1}$ , which leaves the bound on  $\eta$  and  $m_X$  practically unchanged. Furthermore, constraints from limits on CMB distortions and light element abundances from  $^4\text{He}$ -photodisintegration are comparable to the bound from the directly observed diffuse GeV  $\gamma$ -rays [176]. That these crude normalizations lead to values of  $\eta$  in the right range suggests that defect models require less fine tuning than decay rates in scenarios of metastable massive dark matter.

#### 4.4 Results: Neutrino Fluxes

As discussed in Sect. 4.1, in TD scenarios most of the energy is released in the form of EM particles and neutrinos. If the X particles decay into a quark and a lepton, the quark hadronizes mostly into pions and the ratio of energy release into the neutrino versus EM channel is  $r \simeq 0.3$ .

Fig. 5 shows predictions of the total neutrino flux for the same TD model on which Fig. 6 is based. In the absence of neutrino oscillations the electron neutrino and anti-neutrino fluxes are about a factor of 2 smaller than the muon neutrino and anti-neutrino fluxes, whereas the  $\tau$ -neutrino flux is in general negligible. In contrast, if the interpretation of the atmospheric neutrino deficit in terms of nearly maximal mixing of muon and  $\tau$ -neutrinos proves correct, the muon neutrino fluxes shown in Fig. 5 would be maximally mixed with the  $\tau$ -neutrino fluxes. The TD flux component clearly dominates above  $\sim 10^{19} \text{ eV}$ .

In order to translate neutrino fluxes into event rates, one has to fold in the interaction cross sections with matter. At UHEs these cross sections are not directly accessible to laboratory measurements. Resulting uncertainties therefore translate directly to bounds on

neutrino fluxes derived from, for example, the non-detection of UHE muons produced in charged-current interactions. In the following, we will assume the estimate Eq. (7) based on the Standard Model for the charged-current muon-neutrino-nucleon cross section  $\sigma_{\nu N}$  if not indicated otherwise.

For an (energy dependent) ice or water equivalent acceptance  $A(E)$  (in units of volume times solid angle), one can obtain an approximate expected rate of UHE muons produced by neutrinos with energy  $> E$ ,  $R(E)$ , by multiplying  $A(E)\sigma_{\nu N}(E)n_{\text{H}_2\text{O}}$  (where  $n_{\text{H}_2\text{O}}$  is the nucleon density in water) with the integral muon neutrino flux  $\simeq E j_{\nu\mu}$ . This can be used to derive upper limits on diffuse neutrino fluxes from a non-detection of muon induced events. Fig. 5 shows bounds obtained from several experiments: The Frejus experiment derived upper bounds for  $E \gtrsim 10^{12}$  eV from their non-detection of almost horizontal muons with an energy loss inside the detector of more than 140 MeV per radiation length [142]. The AMANDA neutrino telescope has established an upper limit in the TeV-PeV range [52]. The Fly’s Eye experiment derived upper bounds for the energy range between  $\sim 10^{17}$  eV and  $\sim 10^{20}$  eV [88] from the non-observation of deeply penetrating particles. The NASA Goldstone radio telescope has put an upper limit from the non-observation of pulsed radio emission from cascades induced by neutrinos above  $\simeq 10^{20}$  eV in the lunar regolith. The AKENO group has published an upper bound on the rate of near-horizontal, muon-poor air showers [182] (not shown in Fig. 5). Horizontal air showers created by electrons, muons or tau leptons that are in turn produced by charged-current reactions of electron, muon or tau neutrinos within the atmosphere have recently also been pointed out as an important method to constrain or measure UHE neutrino fluxes [63] with next generation detectors.

Clearly, the SLBY model is not only consistent with the constraints discussed in Sect. 4.3, but also with all existing neutrino flux limits within 2-3 orders of magnitude. What, then, are the prospects of detecting UHE neutrino fluxes predicted by TD models? In a  $1 \text{ km}^3 2\pi \text{ sr}$  size detector, the SLBY scenario from Fig. 5, for example, predicts a muon-neutrino event rate of  $\simeq 0.08 \text{ yr}^{-1}$ , and an electron neutrino event rate of  $\simeq 0.05 \text{ yr}^{-1}$  above  $10^{19}$  eV, where “backgrounds” from conventional sources should be negligible. Further, the muon-neutrino event rate above 1 PeV should be  $\simeq 0.6 \text{ yr}^{-1}$ , which could be interesting if conventional sources produce neutrinos at a much smaller flux level. Moreover, the neutrino flux around  $10^{17}$  eV could have a slight enhancement due to neutrinos from muons produced by interactions of UHE photons and electrons with the CMB at high redshift [183], an effect that has not been taken into account in the figures shown here. Of course, above  $\simeq 100$  TeV, instruments using ice or water as detector medium, have to look at downward going muon and electron events due to neutrino absorption in the Earth. However,  $\tau$ -neutrinos obliterate this Earth shadowing effect due to their regeneration from  $\tau$  decays [106]. The presence of  $\tau$ -neutrinos, for example, due to mixing with muon neutrinos, as suggested by recent experimental results from Super-Kamiokande, can therefore lead to an increased upward going event rate [104]. As mentioned in Sect. 2,  $\tau$  neutrinos skimming the Earth at small angles below the horizon can also lead to an increase of sensitivity of fluorescence and ground array detectors [64, 65, 66].

For detectors based on the fluorescence technique such as the HiRes [42] and the Telescope Array [43] (see Sect. 2), the sensitivity to UHE neutrinos is often expressed in terms of an effective aperture  $a(E)$  which is related to  $A(E)$  by  $a(E) = A(E)\sigma_{\nu N}(E)n_{\text{H}_2\text{O}}$ . For



the cross section of Eq. (7), the apertures given in Ref. [42] for the HiRes correspond to  $A(E) \simeq 3 \text{ km}^3 \times 2\pi \text{ sr}$  for  $E \gtrsim 10^{19} \text{ eV}$  for muon neutrinos. The expected acceptance of the ground array component of the Pierre Auger project for horizontal UHE neutrino induced events is  $A(10^{19} \text{ eV}) \simeq 20 \text{ km}^3 \text{ sr}$  and  $A(10^{23} \text{ eV}) \simeq 200 \text{ km}^3 \text{ sr}$  [63], with a duty cycle close to 100%. We conclude that detection of neutrino fluxes predicted by scenarios such as the SLBY scenario shown in Fig. 5 requires running a detector of acceptance  $\gtrsim 10 \text{ km}^3 \times 2\pi \text{ sr}$  over a period of a few years. Apart from optical detection in air, water, or ice, other methods such as acoustical and radio detection [32] (see, e.g., the RICE project [58] for the latter) or even detection from space [46, 47, 48, 49] appear to be interesting possibilities for detection concepts operating at such scales (see Sect. 2). For example, the space based OWL/AirWatch satellite concept would have an aperture of  $\simeq 3 \times 10^6 \text{ km}^2 \text{ sr}$  in the atmosphere, corresponding to  $A(E) \simeq 6 \times 10^4 \text{ km}^3 \text{ sr}$  for  $E \gtrsim 10^{20} \text{ eV}$ , with a duty cycle of  $\simeq 0.08$  [46, 47]. The backgrounds seem to be in general negligible [71, 184]. As indicated by the numbers above and by the projected sensitivities shown in Fig. 5, the Pierre Auger Project and especially the space based AirWatch type projects should be capable of detecting typical TD neutrino fluxes. This applies to any detector of acceptance  $\gtrsim 100 \text{ km}^3 \text{ sr}$ . Furthermore, a 100 day search with a radio telescope of the NASA Goldstone type for pulsed radio emission from cascades induced by neutrinos or cosmic rays in the lunar regolith could reach a sensitivity comparable or better to the Pierre Auger sensitivity above  $\sim 10^{19} \text{ eV}$  [60].

A more model independent estimate [179] for the average event rate  $R(E)$  can be made if the underlying scenario is consistent with observational nucleon and  $\gamma$ -ray fluxes and the bulk of the energy is released above the PP threshold on the CMB. Let us assume that the ratio of energy injected into the neutrino versus EM channel is a constant  $r$ . As discussed in Sect. 4.3, cascading effectively reprocesses most of the injected EM energy into low energy photons whose spectrum peaks at  $\simeq 10 \text{ GeV}$  [171]. Since the ratio  $r$  remains roughly unchanged during propagation, the height of the corresponding peak in the neutrino spectrum should roughly be  $r$  times the height of the low-energy  $\gamma$ -ray peak, i.e., we have the condition  $\max_E [E^2 j_{\nu_\mu}(E)] \simeq r \max_E [E^2 j_\gamma(E)]$ . Imposing the observational upper limit on the diffuse  $\gamma$ -ray flux around  $10 \text{ GeV}$  shown in Fig. 5,  $\max_E [E^2 j_{\nu_\mu}(E)] \lesssim 2 \times 10^3 r \text{ eV cm}^{-2} \text{ sec}^{-1} \text{ sr}^{-1}$ , then bounds the average diffuse neutrino rate above PP threshold on the CMB, giving

$$R(E) \lesssim 0.34 r \left[ \frac{A(E)}{1 \text{ km}^3 \times 2\pi \text{ sr}} \right] \left( \frac{E}{10^{19} \text{ eV}} \right)^{-0.6} \text{ yr}^{-1} \quad (E \gtrsim 10^{15} \text{ eV}), \quad (14)$$

assuming the Standard Model cross section Eq. (7). Comparing this with the flux bounds shown in Fig. 5 results in an upper bound on  $r$ . For example, the Fly's Eye bound translates into  $r \lesssim 20(E/10^{19} \text{ eV})^{0.1}$ . We stress again that TD models are not subject to the Waxman Bahcall bound because the nucleons produced are considerably less abundant than and are not the primaries of produced  $\gamma$ -rays and neutrinos.

In typical TD models such as the one discussed above where primary neutrinos are produced by pion decay,  $r \simeq 0.3$ . However, in TD scenarios with  $r \gg 1$  neutrino fluxes are only limited by the condition that the *secondary*  $\gamma$ -ray flux produced by neutrino interactions with the relic neutrino background be below the experimental limits. In this case the observed EHECR flux would be produced by the Z-burst mechanism discussed in Sect. 3.1. An example for such a scenario is given by X particles exclusively decaying into neutrinos

(although this is not very likely in most particle physics models, but see Ref. [82] and Fig. 8 for a scenario involving topological defects and Ref. [81] for a scenario involving decaying superheavy relic particles, both of which explain the observed EHECR events as secondaries of neutrinos interacting with the primordial neutrino background). Such scenarios predict appreciable event rates above  $\sim 10^{19}$  eV in a  $\text{km}^3$  scale detector, but require unrealistically strong clustering of relic neutrinos (a homogeneous relic neutrino overdensity would make the EGRET constraint only more severe because neutrino interactions beyond  $\sim 50$  Mpc contribute to the GeV  $\gamma$ -ray background but not to the UHECR flux). A detection would thus open the exciting possibility to establish an experimental lower limit on  $r$ . Being based solely on energy conservation, Eq. (14) holds regardless of whether or not the underlying TD mechanism explains the observed EHECR events.

The transient neutrino event rate could be much higher than Eq. (14) in the direction to discrete sources which emit particles in bursts. Corresponding pulses in the EHE nucleon and  $\gamma$ -ray fluxes would only occur for sources nearer than  $\simeq 100$  Mpc and, in case of protons, would be delayed and dispersed by deflection in Galactic and extragalactic magnetic fields [185, 186]. The recent observation of a possible clustering of CRs above  $\simeq 4 \times 10^{19}$  eV by the AGASA experiment [187] might suggest sources which burst on a time scale  $t_b \ll 1$  yr. A burst fluence of  $\simeq r [A(E)/1 \text{ km}^3 \times 2\pi \text{ sr}] (E/10^{19} \text{ eV})^{-0.6}$  neutrino induced events within a time  $t_b$  could then be expected. Associated pulses could also be observable in the GeV – TeV  $\gamma$ -ray flux if the EGMF is smaller than  $\simeq 10^{-15}$  G in a significant fraction of extragalactic space [188].

In contrast to roughly homogeneous sources and/or mechanisms with branching ratios  $r \gg 1$ , in scenarios involving clustered sources such as metastable superheavy relic particles decaying with  $r \sim 1$ , the neutrino flux is comparable to (not significantly larger than) the UHE photon plus nucleon fluxes and thus comparable to the universal cosmogenic flux marked “ $N\gamma$ ” in Fig. 5. This can be understood because the neutrino flux is dominated by the extragalactic contribution which scales with the extragalactic nucleon and  $\gamma$ -ray contribution in exactly the same way as in the unclustered case, whereas the extragalactic contribution to the “visible” flux to be normalized to the UHECR data is much smaller in the clustered case. The resulting neutrino fluxes in these scenarios would thus be much harder to detect even with next generation experiments.

For recent compilations of UHE neutrino flux predictions from astrophysical and TD sources see Refs. [47, 189] and references therein.

## 5 Conclusions

Ultra-high energy cosmic rays have the potential to open a window to and act as probes of new particle physics beyond the Standard Model as well as processes occurring in the early Universe at energies close to the Grand Unification scale. Even if their origin will turn out to be attributable to astrophysical shock acceleration with no new physics involved, they will still be witnesses of one of the most energetic processes in the Universe. The future appears promising and exciting due to the anticipated arrival of several large scale experiments.

## Acknowledgements

I would like to thank all my collaborators in this research field without whose efforts a good part of the work discussed here would not have been possible.

## References

- [1] for a review see, e.g., J. N. Bahcall, Phys. Rept. 333 (2000) 47; for a technical paper on neutrino oscillation parameters including the new SNO data see, e.g., J. N. Bahcall, M. C. Gonzalez-Garcia, C. Pena-Garay, JHEP 0108 (2001) 014.
- [2] see, e.g., J. G. Learned and P. Lipari, proceedings of *Europhysics Neutrino Oscillation Workshop*, Nucl. Phys. Proc. Suppl. 100 (2001) 153.
- [3] Y. Fukuda et al. (Super-Kamiokande collaboration), Phys. Rev. Lett. 81 (1998) 1562.
- [4] for a very recent paper on implications of the neutrinos detected from SN1987A for oscillation parameters see, e.g., M. Kachelriess, A. Strumia, R. Tomas, and J. W. F. Valle, e-print hep-ph/0108100.
- [5] S. Swordy, private communication. The data represent published results of the LEAP, Proton, Akeno, AGASA, Fly's Eye, Haverah Park, and Yakutsk experiments.
- [6] J. Linsley, Phys. Rev. Lett. 10 (1963) 146; Proc. *8th International Cosmic Ray Conference* 4 (1963) 295.
- [7] R. G. Brownlee et al., Can. J. Phys. 46 (1968) S259; M. M. Winn et al., J. Phys. G 12 (1986) 653; see also <http://www.physics.usyd.edu.au/hienergy/sugar.html>.
- [8] See, e.g., M. A. Lawrence, R. J. O. Reid, and A. A. Watson, J. Phys. G Nucl. Part. Phys. 17 (1991) 733, and references therein; see also <http://ast.leeds.ac.uk/haverah/hav-home.html>.
- [9] Proc. International Symposium on *Astrophysical Aspects of the Most Energetic Cosmic Rays*, eds. M. Nagano and F. Takahara (World Scientific, Singapore, 1991)
- [10] Proc. of International Symposium on *Extremely High Energy Cosmic Rays: Astrophysics and Future Observatories*, ed. M. Nagano (Institute for Cosmic Ray Research, Tokyo, 1996).
- [11] N. N. Efimov et al., Ref. [9], p. 20; B. N. Afanasiev, in Ref. [10], p. 32.
- [12] D. J. Bird et al., Phys. Rev. Lett. 71 (1993) 3401; Astrophys. J. 424 (1994) 491; *ibid.* 441 (1995) 144.
- [13] N. Hayashida et al., Phys. Rev. Lett. 73 (1994) 3491; S. Yoshida et al., Astropart. Phys. 3 (1995) 105; M. Takeda et al., Phys. Rev. Lett. 81 (1998) 1163; see also <http://icrsun.icrr.u-tokyo.ac.jp/as/project/agasa.html>.

- [14] V. S. Berezhinsky, S. V. Bulanov, V. A. Dogiel, V. L. Ginzburg, and V. S. Ptuskin, *Astrophysics of Cosmic Rays* (North-Holland, Amsterdam, 1990).
- [15] T. K. Gaisser, *Cosmic Rays and Particle Physics*, Cambridge University Press (Cambridge, England, 1990)
- [16] G. Sigl, *Science* 291 (2001) 73.
- [17] M. Nagano, A. A. Watson, *Rev. Mod. Phys.* 72 (2000) 689.
- [18] J. W. Cronin, *Rev. Mod. Phys.* 71 (1999) S165; A. V. Olinto, *Phys. Rept.* 333-334 (2000) 329; X. Bertou, M. Boratav, and A. Letessier-Selvon, *Int. J. Mod. Phys. A15* (2000) 2181;
- [19] P. Bhattacharjee and G. Sigl, *Phys. Rept.* 327 (2000) 109.
- [20] A. M. Hillas, *Ann. Rev. Astron. Astrophys.* 22 (1984) 425.
- [21] G. Sigl, D. N. Schramm, and P. Bhattacharjee, *Astropart. Phys.* 2 (1994) 401.
- [22] C. A. Norman, D. B. Melrose, and A. Achterberg, *Astrophys. J.* 454 (1995) 60.
- [23] P. L. Biermann, *J. Phys. G: Nucl. Part. Phys.* 23 (1997) 1.
- [24] J. G. Kirk and P. Duffy, *J. Phys. G: Nucl. Part. Phys.* 25 (1999) R163.
- [25] K. Greisen, *Phys. Rev. Lett.* 16 (1966) 748.
- [26] G. T. Zatsepin and V. A. Kuzmin, *Pis'ma Zh. Eksp. Teor. Fiz.* 4 (1966) 114 [*JETP Lett.* 4 (1966) 78].
- [27] F. W. Stecker, *Phys. Rev. Lett.* 21 (1968) 1016.
- [28] J. L. Puget, F. W. Stecker, and J. H. Bredekamp, *Astrophys. J.* 205 (1976) 638.
- [29] L. N. Epele and E. Roulet, *Phys. Rev. Lett.* 81 (1998) 3295; *J. High Energy Phys.* 9810 (1998) 009; F. W. Stecker, *Phys. Rev. Lett.* 81 (1998) 3296; F. W. Stecker and M. H. Salamon, *Astrophys. J.* 512 (1999) 521.
- [30] J. W. Elbert, and P. Sommers, *Astrophys. J.* 441 (1995) 151.
- [31] E. Boldt and P. Ghosh, in *Mon. Not. R. Astron. Soc.* 307 (1999) 491.
- [32] T. K. Gaisser, F. Halzen, and T. Stanev, *Phys. Rept.* 258 (1995) 173.
- [33] F. Halzen, e-print astro-ph/9810368, lectures presented at the TASI School, July 1998; e-print astro-ph/9904216, talk presented at the *17th International Workshop on Weak Interactions and Neutrinos*, Cape Town, South Africa, January 1999;

- [34] R. A. Ong, Phys. Rept. 305 (1998) 95; M. Catanese and T. C. Weekes, e-print astro-ph/9906501, invited review, Publ. Astron. Soc. of the Pacific, Vol. 111, issue 764 (1999) 1193.
- [35] K. Mannheim, Rev. Mod. Astron. 12 (1999) 101.
- [36] E. Waxman and J. Bahcall, Phys. Rev. D. 59 (1999) 023002; J. Bahcall and E. Waxman, Phys. Rev. D 64 (2001) 023002.
- [37] Proceedings of the *19th Texas Symposium on Relativistic Astrophysics* (Paris, France, 1998).
- [38] K. Mannheim, R. J. Protheroe, and J. P. Rachen, Phys. Rev. D 63 (2001) 023003; J. P. Rachen, R. J. Protheroe, and K. Mannheim, e-print astro-ph/9908031, in [37].
- [39] See, e.g., S. Petrera, Nuovo Cimento 19C (1996) 737.
- [40] S. Yoshida and H. Dai, J. Phys. G 24 (1998) 905; P. Sokolsky, *Introduction to Ultra-high Energy Cosmic Ray Physics* (Addison Wesley, Redwood City, California, 1989); P. Sokolsky, P. Sommers, and B. R. Dawson, Phys. Rept. 217 (1992) 225; M. V. S. Rao and B. V. Sreekantan, *Extensive Air Showers* (World Scientific, Singapore, 1998).
- [41] Proc. *24th International Cosmic Ray Conference* (Istituto Nazionale Fisica Nucleare, Rome, Italy, 1995)
- [42] S. C. Corbató et al., Nucl. Phys. B (Proc. Suppl.) 28B (1992) 36; D. J. Bird et al., in [41], Vol. 2, 504; Vol. 1,750; M. Al-Seady et al., in [10], p. 191; see also <http://hires.physics.utah.edu/>.
- [43] M. Teshima et al., Nucl. Phys. B (Proc. Suppl.) 28B (1992), 169; M. Hayashida et al., in [10], p. 205; see also <http://www-ta.icrr.u-tokyo.ac.jp/>.
- [44] J. W. Cronin, Nucl. Phys. B (Proc. Suppl.) 28B (1992) 213; The Pierre Auger Observatory Design Report (2nd edition), March 1997; see also <http://http://www.auger.org/> and <http://www-lpnhep.in2p3.fr/auger/welcome.html>.
- [45] Proc. *25th International Cosmic Ray Conference*, eds.: M. S. Potgieter et al. (Durban, 1997).
- [46] J. F. Ormes et al., in [45], Vol. 5, 273; Y. Takahashi et al., in [10], p. 310; see also <http://lheawww.gsfc.nasa.gov/docs/gamcosray/hecr/OWL/>.
- [47] D. B. Cline and F. W. Stecker, OWL/AirWatch science white paper, e-print astro-ph/0003459.
- [48] See <http://www.ifcai.pa.cnr.it/lfcai/euso.html>.
- [49] J. Linsley, in Ref. [45], Vol. 5, 381; *ibid.*, 385; P. Attinà et al., *ibid.*, 389; J. Forbes et al., *ibid.*, 273; see also <http://www.ifcai.pa.cnr.it/lfcai/airwatch.html>.

- [50] Proc. of *Workshop on Observing Giant Cosmic Ray Air Showers from  $> 10^{20}$  eV Particles from Space*, eds. J. F. Krizmanic, J. F. Ormes, and R. E. Streitmatter (AIP Conference Proceedings 433, 1997).
- [51] See <http://dumand.phys.washington.edu/~dumand/>.
- [52] For general information see <http://amanda.berkeley.edu/>; see also F. Halzen, *New Astron. Rev* 42 (1999) 289; for newest status see, e.g., G. C. Hill et al. (Amanda Collaboration), e-print astro-ph/0106064.
- [53] For general information see <http://www.ifh.de/baikal/baikalhome.html>; also see Baikal Collaboration, e-print astro-ph/9906255, talk given at the *8th Int. Workshop on Neutrino Telescopes*, Venice, Feb 1999.
- [54] For general information see <http://antares.in2p3.fr/antares/antares.html>; see also S. Basa, in [37] (e-print astro-ph/9904213); ANTARES Collaboration, e-print astro-ph/9907432.
- [55] For general information see <http://www.roma1.infn.it/nestor/nestor.html>.
- [56] For general information see <http://www.ps.uci.edu/~icecube/workshop.html>; see also F. Halzen, *Am. Astron. Soc. Meeting* 192 (1998) # 62 28; AMANDA collaboration, e-print astro-ph/9906205, talk presented at the *8th Int. Workshop on Neutrino Telescopes*, Venice, Feb 1999.
- [57] Proceedings of *First International Workshop on Radio Detection of High-Energy Particles*, Amer. Inst. of Phys., 2001, and at <http://www.physics.ucla.edu/~moonemp/radhhep/workshop.html>.
- [58] For general information see <http://kuhep4.phsx.ukans.edu/~iceman/index.html>.
- [59] Proc. *26th International Cosmic Ray Conference*, (Utah, 1999).
- [60] P. W. Gorham, K. M. Liewer, and C. J. Naudet, e-print astro-ph/9906504, in [59]; P. W. Gorham et al., e-print astro-ph/0102435, in Ref. [57].
- [61] J. Alvarez-Muniz and E. Zas, e-print astro-ph/0102173, in Ref. [57].
- [62] N. G. Lehtinen et al., e-print astro-ph/0104033.
- [63] J. J. Blanco-Pillado, R. A. Vázquez, and E. Zas, *Phys. Rev. Lett.* 78 (1997) 3614; K. S. Capelle, J. W. Cronin, G. Parente, and E. Zas, *Astropart. Phys.* 8 (1998) 321; A. Letessier-Selvon, e-print astro-ph/0009444.
- [64] D. Fargion, e-print astro-ph/0002453, astro-ph/0101565.
- [65] X. Bertou et al., e-print astro-ph/0104452.
- [66] J. L. Feng, P. Fisher, F. Wilczek, and T. M. Yu, e-print hep-ph/0105067; A. Kusenko and T. Weiler, e-print hep-ph/0106071.

- [67] J. G. Learned, *Phil. Trans. Roy. Soc. London A* 346 (1994) 99.
- [68] T. J. Weiler, *Phys. Rev. Lett.* 49 (1982) 234; *Astrophys. J.* 285 (1984) 495.
- [69] E. Roulet, *Phys. Rev. D* 47 (1993) 5247.
- [70] S. Yoshida, *Astropart. Phys.* 2 (1994) 187.
- [71] S. Yoshida, H. Dai, C. C. H. Jui, and P. Sommers, *Astrophys. J.* 479 (1997) 547.
- [72] D. Seckel, *Phys. Rev. Lett.* 80 (1998) 900.
- [73] D. A. Dicus and W. W. Repko, *Phys. Rev. Lett.* 79 (1997) 569.
- [74] M. Harris, J. Wang, and V. L. Teplitz, e-print astro-ph/9707113.
- [75] P. Bhattacharjee, C. T. Hill, and D. N. Schramm, *Phys. Rev. Lett.* 69 (1992) 567.
- [76] R. Cowsik and J. McClelland, *Phys. Rev. Lett.* 29 (1972) 669; *Astrophys. J.* 180 (1973) 7; R. Cowsik and P. Ghosh, *Astrophys. J.* 317 (1987) 26.
- [77] D. Fargion, B. Mele, and A. Salis, *Astrophys. J.* 517 (1999) 725.
- [78] T. J. Weiler, *Astropart. Phys.* 11 (1999) 303.
- [79] E. Waxman, e-print astro-ph/9804023.
- [80] S. Yoshida, G. Sigl, and S. Lee, *Phys. Rev. Lett.* 81 (1998) 5505.
- [81] G. Gelmini and A. Kusenko, *Phys. Rev. Lett.* 84 (2000) 1378; G. Gelmini, e-print hep-ph/0005263, to appear in *Proceedings of 4th International Symposium on Sources and Detection of Dark Matter in the Universe*, Feb. 2000, Marina del Rey.
- [82] G. Sigl, S. Lee, P. Bhattacharjee, and S. Yoshida, *Phys. Rev. D* 59 (1999) 043504.
- [83] R. J. Protheroe and P. L. Biermann, *Astropart. Phys.* 6 (1996) 45.
- [84] P. Sreekumar et al., *Astrophys. J.* 494 (1998) 523.
- [85] A. Karle et al., *Phys. Lett. B* 347 (1995) 161.
- [86] J. Matthews et al., *Astrophys. J.* 375 (1991) 202.
- [87] M. C. Chantell et al., *Phys. Rev. Lett.* 79 (1997) 1805.
- [88] R. M. Baltrusaitis et al., *Astrophys. J.* 281 (1984) L9; *Phys. Rev. D* 31 (1985) 2192.
- [89] G. Sigl and S. Lee, in [41], Vol. 3, 356.
- [90] J. J. Blanco-Pillado, R. A. Vázquez, E. Zas, *Phys. Rev. D* 61 (2000) 123003.
- [91] G. Gelmini and A. Kusenko, *Phys. Rev. Lett.* 82 (1999) 5202.

- [92] P. B. Pal and K. Kar, Phys. Lett. B 451 (1999) 136.
- [93] I. Affleck and M. Dine, Nucl. Phys. B 249 (1985) 361.
- [94] See, e.g., F. W. Stecker, C. Done, M. Salamon, and P. Sommers, Phys. Rev. Lett. 66 (1991) 2697; A. P. Szabo and R. J. Protheroe, Astropart. Phys. 2 (1994) 375; F. W. Stecker and M. H. Salamon, Space. Sc. Rev. 75 (1996) 341; V. S. Berezinsky, Nucl. Phys. B (Proc. Suppl.) 38 (1995) 363.
- [95] K. Mannheim, Astropart. Phys. 3 (1995) 295.
- [96] F. Halzen and E. Zas, Astrophys. J. 488 (1997) 669.
- [97] R. Protheroe, in *Accretion Phenomena and Related Outflows*, Vol. 163 of IAU Colloquium, eds. D. Wickramasinghe, G. Bicknell, and L. Ferrario (Astron. Soc. of the Pacific, 1997), p. 585.
- [98] R. Protheroe, e-print astro-ph/9809144, invited talk at Neutrino 98, Takayama 4-9 June 1998.
- [99] E. Waxman and J. Bahcall, Phys. Rev. D. 59 (1999) 023002.
- [100] F. W. Stecker, Astrophys. J. 228 (1979) 919.
- [101] C. T. Hill and D. N. Schramm, Phys. Lett. B 131 (1983) 247.
- [102] Z. Fodor, S. D. Katz, e-print hep-ph/0105064; hep-ph/0105336.
- [103] Proceedings of *VERITAS Workshop on TeV Astrophysics of Extragalactic Sources*, eds. M. Catanese, J. Quinn, T. Weekes, Astropart. Phys. Vol. 11 (1999).
- [104] K. Mannheim, in [103], Astropart. Phys. 11 (1999) 49.
- [105] J. G. Learned and S. Pakvasa, Astropart. Phys. 3 (1995) 267.
- [106] F. Halzen and D. Saltzberg, Phys. Rev. Lett. 81 (1998) 4305.
- [107] R. Horvat, Phys. Rev. D 59 (1999) 123003.
- [108] P. Keränen, J. Maalampi, and J. T. Peltoniemi, Phys. Lett. B 461 (1999) 230.
- [109] G. M. Frichter, D. W. McKay, and J. P. Ralston, Phys. Rev. Lett. 74 (1995) 1508.
- [110] R. Gandhi, C. Quigg, M. H. Reno, and I. Sarcevic, Astropart. Phys. 5 (1996) 81; Phys. Rev. D 58 (1998) 093009.
- [111] M. Glück, S. Kretzer, and E. Reya, Astropart. Phys. 11 (1999) 327.
- [112] M. Derick et al. (ZEUS collaboration), Phys. Lett. B 316 (1993) 412; Z. Phys. C 65 (1995) 379; I. Abt et al. (H1 collaboration), Nucl. Phys. B407 (1993) 515; T. Ahmed et al. (H1 collaboration) Nucl. Phys. B 439 (1995) 471.



- [113] G. Gelmini, P. Gondolo, and G. Varieschi, *Phys. Rev. D* 61 (2000) 056011.
- [114] J. Kwiecinski, A. D. Martin, and A. Stasto, *Phys. Rev. D* 59 (1999) 093002.
- [115] D. A. Dicus, S. Kretzer, W. W. Repko, and C. Schmidt, *Phys. Lett. B* 514 (2001) 103.
- [116] M. Kachelriess and M. Plümacher, private communication.
- [117] G. Sigl, *Phys. Rev. D* 57 (1998) 3786.
- [118] V. A. Naumov and L. Perrone, *Astropart. Phys.* 10 (1999) 239.
- [119] P. Jain, J. P. Ralston, and G. M. Frichter, *Astropart. Phys.* 12 (1999) 193.
- [120] J. Bordes et al., *Astropart. Phys.* 8 (1998) 135; in *Beyond the Standard Model. From Theory to Experiment* (Valencia, Spain, 13-17 October 1997), eds. I. Antoniadis, L. E. Ibanez, and J. W. F. Valle (World Scientific, Singapore, 1998), p. 328 (e-print hep-ph/9711438).
- [121] G. Sigl, *Nucl. Phys. B* 87 (Proc. Suppl.) (2000) 439, Proceedings of TAUP 99, eds.: M. Froissart, J. Dumarchez, and D. Vignaud, College de France, Paris, 6-10 September 1999.
- [122] P. Jain, D. W. McKay, S. Panda, and J. P. Ralston, *Phys. Lett. B* 484 (2000) 267; J. P. Ralston, P. Jain, D. W. McKay, S. Panda, e-print hep-ph/0008153.
- [123] G. Burdman, F. Halzen, and R. Gandhi, *Phys. Lett. B* 417 (1998) 107.
- [124] G. Domokos and S. Kovesi-Domokos, *Phys. Rev. Lett.* 82 (1999) 1366.
- [125] N. Arkani-Hamed, S. Dimopoulos, and G. Dvali, *Phys. Lett. B* 429 (1998) 263; I. Antoniadis, N. Arkani-Hamed, S. Dimopoulos, and G. Dvali, *Phys. Lett. B* 436 (1998) 257; N. Arkani-Hamed, S. Dimopoulos, and G. Dvali, *Phys. Rev. D* 59 (1999) 086004.
- [126] S. Nussinov and R. Shrock, *Phys. Rev. D* 59 (1999) 105002; *Phys. Rev. D* 64 (2001) 047702
- [127] M. Kachelrieß and M. Plümacher, *Phys. Rev. D* 62 (2000) 103006.
- [128] L. Anchordoqui et al., *Phys. Rev. D* 63 (2001) 124009.
- [129] see, e.g., C. Spiering, *Nucl. Phys. Proc. Suppl.* 91 (2000) 445.
- [130] C. Tyler, A. Olinto, and G. Sigl, *Phys. Rev. D.* (2001) 63 055001.
- [131] J. Alvarez-Muniz, F. Halzen, T. Han, and D. Hooper, e-print hep-ph/0107057.
- [132] see, e.g., S. Cullen, M. Perelstein, and M. E. Peskin, *Phys. Rev. D* 62 (2000) 055012, and references therein; I. Antoniadis and K. Benakli, e-print hep-ph/0108174.
- [133] S. Dimopoulos and R. Emparan, e-print hep-ph/0108060, and references therein.

- [134] J. L. Feng and A. D. Shapere, e-print hep-ph/0109106.
- [135] F. Cornet, J. L. Illana, and M. Masip, Phys. Rev. Lett. 86 (2001) 4235.
- [136] S. Cullen and M. Perelstein, Phys. Rev. Lett. 83 (1999) 268; V. Barger, T. Han, C. Kao, and R.-J. Zhang, Phys. Lett. B 461 (1999) 34.
- [137] S. Hannestad and G. Raffelt, Phys. Rev. Lett. 87 (2001) 051301.
- [138] S. Hannestad, Phys. Rev. D 64 (2001) 023515.
- [139] see, e.g., K. R. Dienes, e-print hep-ph/0108115.
- [140] J. C. Long, H. W. Chan, and J. C. Price, Nucl. Phys. B 539 (1999) 23.
- [141] D. A. Morris and A. Ringwald, Astropart. Phys. 2 (1994) 43.
- [142] W. Rhode et al., Astropart. Phys. 4 (1996) 217.
- [143] P. Lipari, Astropart. Phys. 1 (1993) 195.
- [144] R. J. Protheroe and P. A. Johnson, Astropart. Phys. 4 (1996) 253, and erratum ibid. 5 (1996) 215.
- [145] H. Goldberg and T. J. Weiler, Phys. Rev. D 59 (1999) 113005.
- [146] G. R. Farrar and P. L. Biermann, Phys. Rev. Lett. 81 (1998) 3579.
- [147] C. Hoffman, Phys. Rev. Lett. 83 (1999) 2471.
- [148] G. R. Farrar and P. L. Biermann, Phys. Rev. Lett. 83 (1999) 2472.
- [149] G. Sigl, D. F. Torres, L. A. Anchordoqui, and G. E. Romero, Phys. Rev. D 63 (2001) 081302.
- [150] A. Virmani et al., e-print astro-ph/0010235.
- [151] P. G. Tinyakov and I. I. Tkachev, e-print astro-ph/0102476.
- [152] see, e.g., T. Vachaspati, Contemp. Phys. 39 (1998) 225.
- [153] for a brief review see V. Kuzmin and I. Tkachev, Phys. Rept. 320 (1999) 199.
- [154] see, e.g., P. Bhattacharjee and N. C. Rana, Phys. Lett. B 246 (1990) 365.
- [155] V. Berezhinsky and A. Vilenkin, Phys. Rev. Lett. 79 (1997) 5202.
- [156] P. Bhattacharjee and G. Sigl, Phys. Rev. D 51 (1995) 4079.
- [157] Yu. L. Dokshitzer, V. A. Khoze, A. H. Müller, and S. I. Troyan, *Basics of Perturbative QCD* (Editions Frontieres, Singapore, 1991).

- [158] V. Berezhinsky and M. Kachelrieß, Phys. Lett. B 434 (1998) 61.
- [159] M. Birkel and S. Sarkar, Astropart. Phys. 9 (1998) 297; S. Sarkar, S. Sarkar and R. Toldra, e-print hep-ph/0108098.
- [160] V. Berezhinsky and M. Kachelrieß, Phys. Rev. D 63 (2001) 034007.
- [161] S. Lee, Phys. Rev. D 58 (1998) 043004.
- [162] T. J. Weiler, Phys. Rev. Lett. 49 (1982) 234; Astrophys. J. 285 (1984) 495; E. Roulet, Phys. Rev. D 47 (1993) 5247; S. Yoshida, Astropart. Phys. 2 (1994) 187.
- [163] see, e.g., P. J. E. Peebles, *Principles of Physical Cosmology*, Princeton University Press, New Jersey, 1993.
- [164] R. V. Konoplich and S. G. Rubin, JETP Lett. 72 (2000) 97, A. Goyal, A. Gupta, and N. Mahajan, Phys. Rev. D 63 (2001) 043003.
- [165] F. A. Aharonian, P. Bhattacharjee, and D. N. Schramm, Phys. Rev. D 46 (1992) 4188.
- [166] T. A. Clark, L. W. Brown, and J. K. Alexander, Nature 228 (1970) 847.
- [167] D. Ryu, H. Kang, and P. L. Biermann, Astron. Astrophys. 335 (1998) 19.
- [168] See, e.g., S. Biller et al., Phys. Rev. Lett. 80 (1998) 2992; T. Stanev and A. Franceschini, Astrophys. J. 494 (1998) L159; F. W. Stecker and O. C. de Jager, Astron. Astrophys. 334 (1998) L85; J. R. Primack, R. S. Somerville, J. S. Bullock, J. E. G. Devriendt, e-print astro-ph/0011475, Proceedings of the International Symposium on Gamma-Ray Astronomy, Heidelberg, June 2000, eds F. Aharonian and H. Völk, AIP Conf. Proc.
- [169] R. J. Protheroe and T. Stanev, Phys. Rev. Lett. 77 (1996) 3708; erratum, ibid. 78 (1997) 3420.
- [170] G. Sigl, S. Lee, D. N. Schramm, and P. Bhattacharjee, Science 270 (1995) 1977.
- [171] P. S. Coppi and F. A. Aharonian, Astrophys. J. 487 (1997) L9.
- [172] R. Mukherjee and J. Chiang, Astropart. Phys. 11 (1999) 213.
- [173] V. Berezhinsky, M. Kachelrieß, and A. Vilenkin, Phys. Rev. Lett. 79 (1997) 4302.
- [174] S. Lee, A. V. Olinto, and G. Sigl, Astrophys. J. 455 (1995) L21.
- [175] C. T. Hill, Nucl. Phys. B 224 (1983) 469.
- [176] G. Sigl, K. Jedamzik, D. N. Schramm, and V. Berezhinsky, Phys. Rev. D 52 (1995) 6682.
- [177] O. E. Kalashev, V. A. Kuzmin, and D. V. Semikoz, e-print astro-ph/9911035; O. E. Kalashev, V. A. Kuzmin, D. V. Semikoz, and G. Sigl, in preparation.

- [178] F. Halzen, R. V'azques, T. Stanev, and H. P. Vankov, *Astropart. Phys.* 3 (1995) 151; M. Ave et al., *Phys. Rev. Lett.* 85 (2000) 2244; E. Zas, e-print astro-ph/0011416.
- [179] G. Sigl, S. Lee, D. N. Schramm, and P. S. Coppi, *Phys. Lett. B* 392 (1997) 129.
- [180] G. R. Vincent, N. D. Antunes, and M. Hindmarsh, *Phys. Rev. Lett.* 80 (1998) 2277; G. R. Vincent, M. Hindmarsh, and M. Sakellariadou, *Phys. Rev. D* 56 (1997) 637.
- [181] U. F. Wichoski, J. H. MacGibbon, and R. H. Brandenberger, e-print hep-ph/9805419; U. F. Wichoski, R. H. Brandenberger, and J. H. MacGibbon, e-print hep-ph/9903545, *Proceedings of 2nd Meeting on New Worlds in Astroparticle Physics* (Faro, Portugal, 3-5 Sep 1998), eds. A. Mourao, M. Pimenta and P. Sa (World Scientific, Singapore, 1999).
- [182] M. Nagano et al., *J. Phys. G* 12 (1986) 69.
- [183] M. Postma, *Phys. Rev. D* 64 (2001) 023001; see also H. Athar, G.-L. Lin, and J.-J. Tseng, hep-ph/0104185.
- [184] P. B. Price, *Astropart. Phys.* 5 (1996) 43.
- [185] E. Waxman and J. Miralda-Escudé, *Astrophys. J.* 472 (1996) L89.
- [186] M. Lemoine, G. Sigl, A. V. Olinto, and D.N. Schramm, *Astrophys. J.* 486 (1997) L115.
- [187] N. Hayashida et al., *Phys. Rev. Lett.* 77 (1996) 1000; Y. Uchihori et al, *Astropart. Phys.* 13 (2000) 151.
- [188] E. Waxman and P. S. Coppi, *Astrophys. J.* 464 (1996) L75.
- [189] R. Protheroe, e-print astro-ph/9809144, invited talk at Neutrino 98, Takayama 4-9 June 1998; M. Roy and H. J. Crawford, e-print astro-ph/9808170, submitted to *Astropart. Phys.*; R. Ghandi, *Nucl. Phys. Proc. Suppl.* 91 (2000) 453.

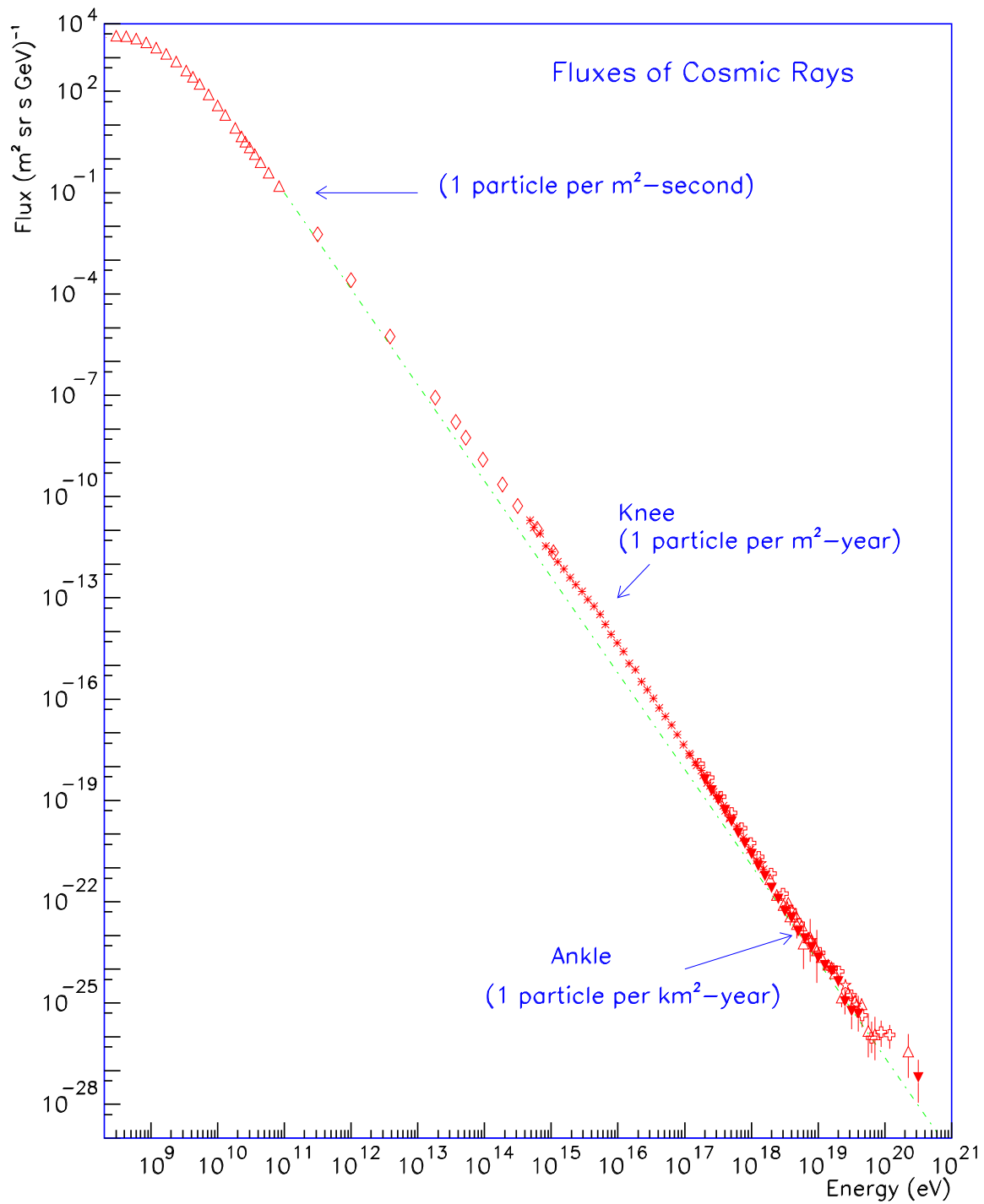


Figure 1: The cosmic ray all particle spectrum [5]. Approximate integral fluxes are also shown

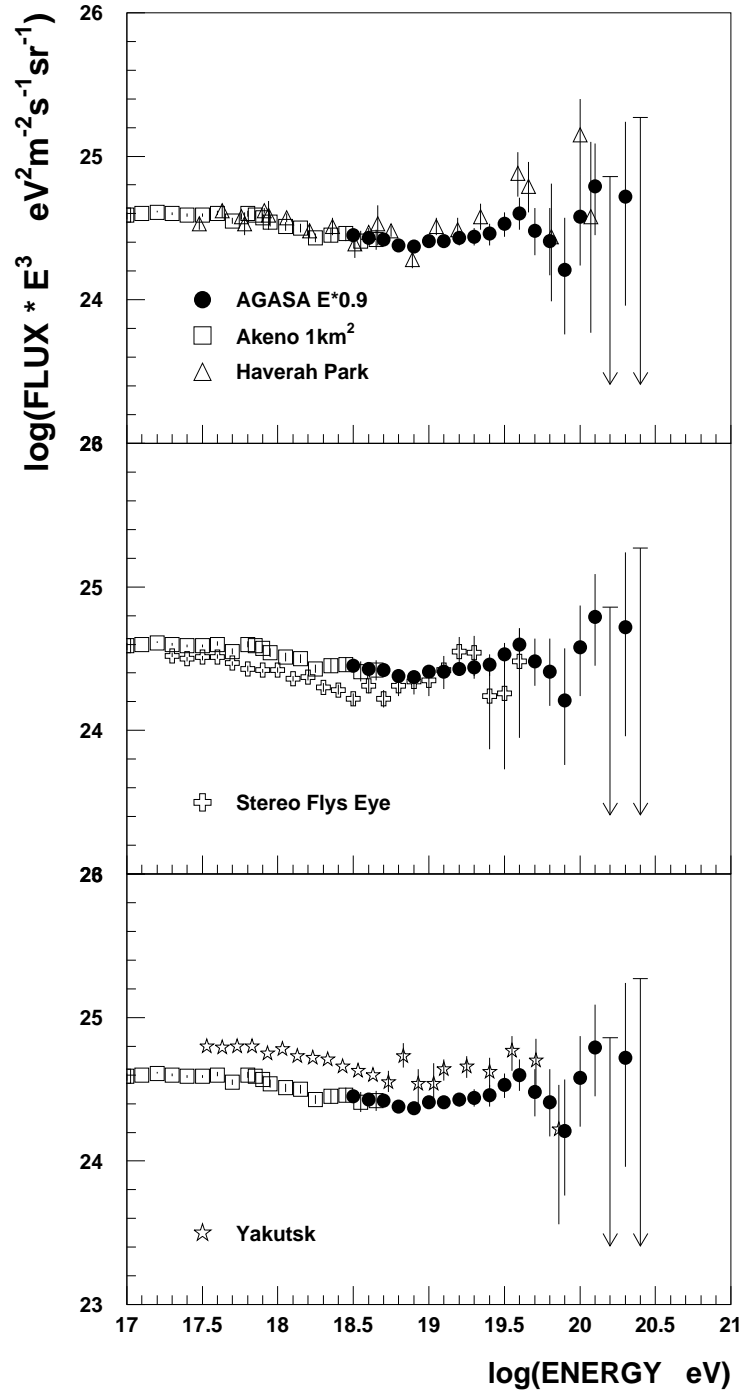


Figure 2: The cosmic ray spectrum above  $10^{17}$  eV (from Ref [17]). The “ankle” is visible at  $E \simeq 5 \times 10^{18}$  eV.

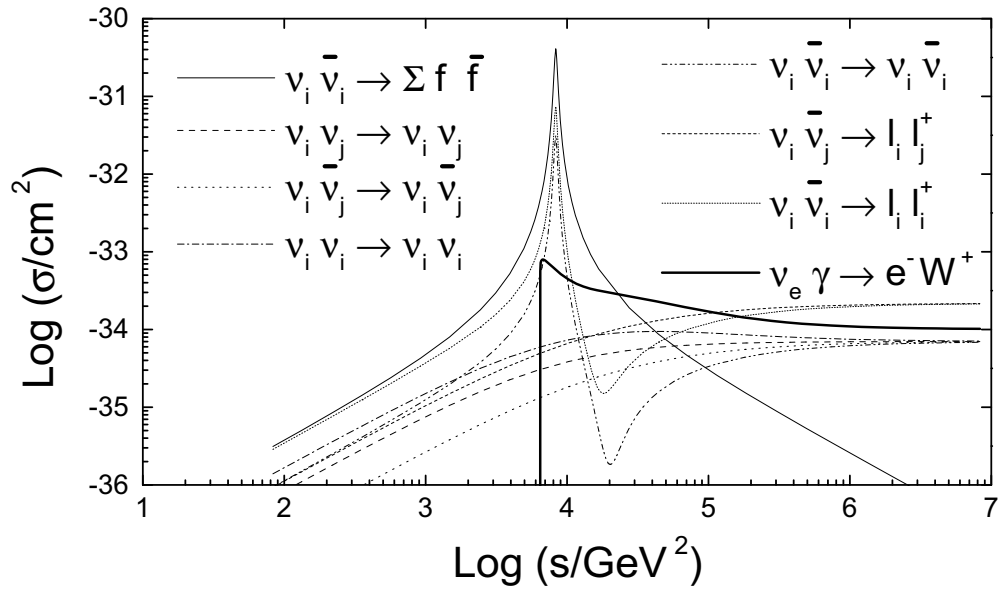


Figure 3: Various cross sections relevant for neutrino propagation as a function of  $s$  [69, 72]. The sum  $\sum_j f_j \bar{f}_j$  does not include  $f_j = \nu_i, l_i, t, W,$  or  $Z$ . (From Ref. [72]).

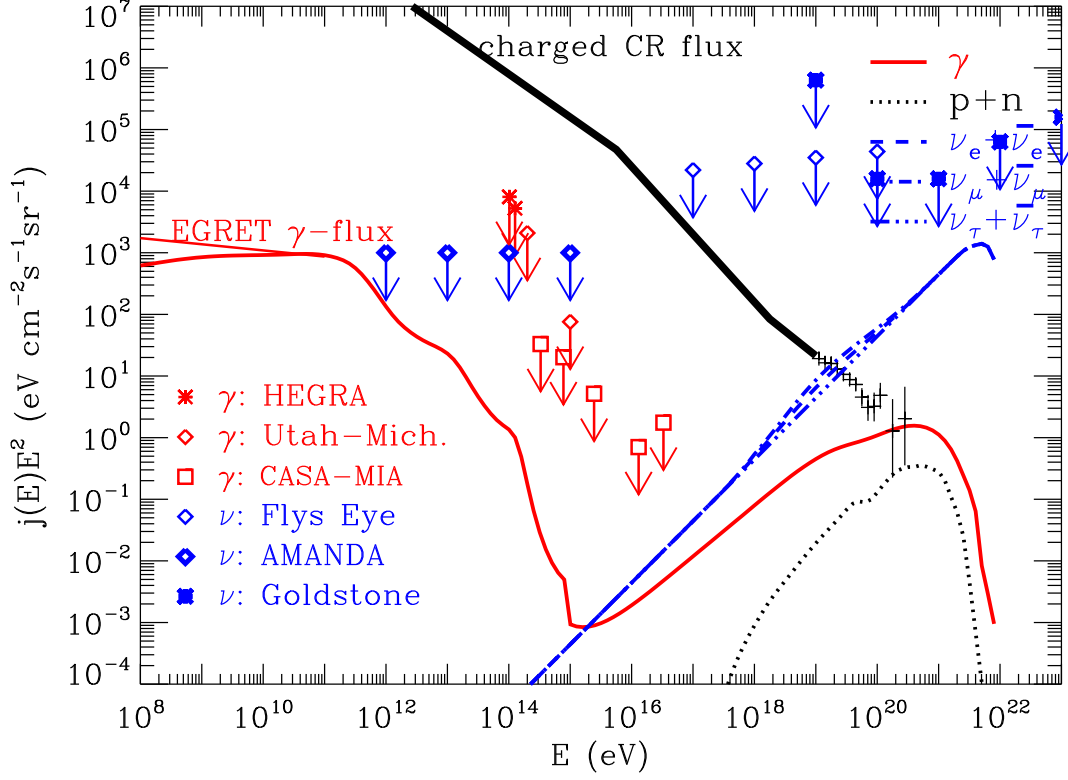


Figure 4: Fluxes of neutrinos (dashed and dashed-dotted, as indicated),  $\gamma$ -rays (solid), and nucleons (dotted) predicted by the Z-burst mechanism for  $m_{\nu_e} = 0.1$  eV,  $m_{\nu_\mu} = m_{\nu_\tau} = 1$  eV, for homogeneously distributed sources emitting neutrinos with an  $E^{-1}$  spectrum (equal for all flavors) up to  $10^{22}$  eV and an  $E^{-2}$   $\gamma$ -ray spectrum of equal power up to 100 TeV. Injection rates were assumed comovingly constant up to  $z = 2$ . The relic neutrino overdensity was assumed to be 200 over 5 Mpc. The calculation used the code described in Ref. [82] and assumed the lower limit of the universal radio background [83] and a vanishing extragalactic magnetic field. 1 sigma error bars are the combined data from the Haverah Park [8], the Fly’s Eye [12], and the AGASA [13] experiments above  $10^{19}$  eV. Also shown are piecewise power law fits to the observed charged CR flux (thick solid line) and the EGRET measurement of the diffuse  $\gamma$ -ray flux between 30 MeV and 100 GeV [84] (solid line on left margin). Points with arrows represent upper limits on the  $\gamma$ -ray flux from the HEGRA [85], the Utah-Michigan [86], and the CASA-MIA [87] experiments, and on the neutrino flux from the Fly’s Eye experiment [88], the Goldstone radio telescope [60], and the AMANDA neutrino telescope [52], as indicated (see text and Ref. [19] for more details).



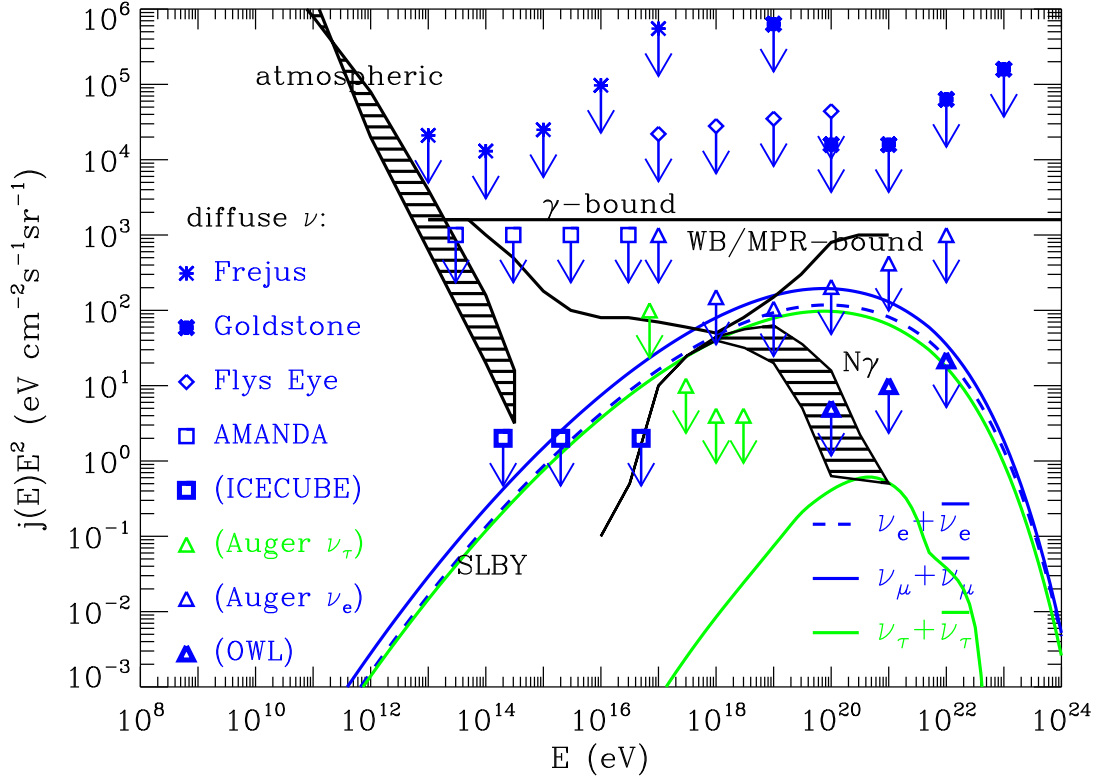


Figure 5: Various neutrino flux predictions and experimental upper limits or projected sensitivities. Shown are upper limits from the Frejus underground detector [142], the Fly’s Eye experiment [88], the Goldstone radio telescope [60], and the Antarctic Muon and Neutrino Detector Array (AMANDA) neutrino telescope [52], as well as projected neutrino flux sensitivities of ICECUBE, the planned kilometer scale extension of AMANDA [56], the Pierre Auger Project [63] (for electron and tau neutrinos separately) and the proposed space based OWL [46] concept. Neutrino fluxes are shown for the atmospheric neutrino background [143] (hatched region marked “atmospheric”), for EHECR interactions with the CMB [144] (“ $N\gamma$ ”, dashed range indicating typical uncertainties for moderate source evolution), and for the “top-down” model (marked “SLBY”) corresponding to Fig. 7 of Sect. 4 below, where EHECR and neutrinos are produced by decay of superheavy relics. The top-down fluxes are shown for electron-, muon, and tau-neutrinos separately, assuming no (lower  $\nu_\tau$ -curve) and maximal  $\nu_\mu - \nu_\tau$  mixing (upper  $\nu_\tau$ -curve, which would then equal the  $\nu_\mu$ -flux), respectively. The Waxman-Bahcall bound in the version of Mannheim, Protheroe, and Rachen [38] (“WB/MPR-bound”) for sources optically thin for the proton primaries, and the  $\gamma$ -ray bound (“ $\gamma$ -bound”) are also shown.

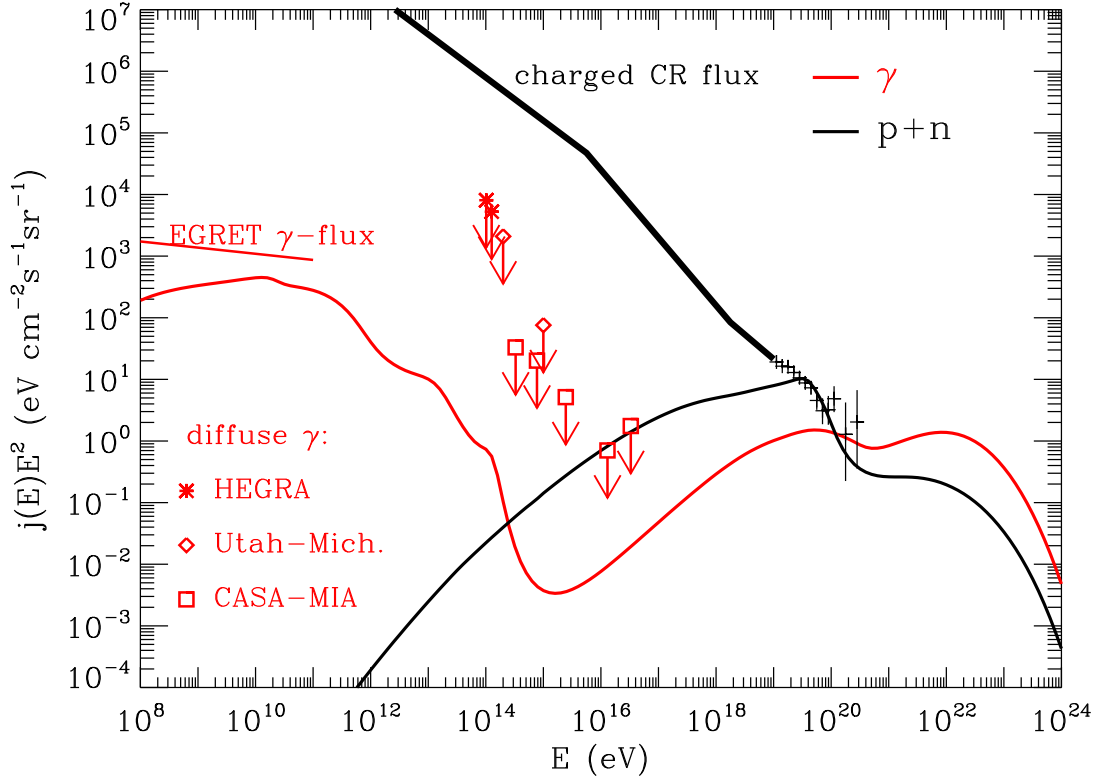


Figure 6: Predictions for the differential fluxes of  $\gamma$ -rays (solid line) and protons and neutrons (dotted line) in a TD model characterized by  $p = 1$ ,  $m_X = 10^{16}$  GeV, and the decay mode  $X \rightarrow q + q$ , assuming the supersymmetric modification of the fragmentation function [158], with a fraction of about 10% nucleons. The defects have been assumed to be homogeneously distributed. The calculation used the code described in Ref. [82] and assumed an intermediate URB estimate from Ref. [83] and an EGMF  $\ll 10^{-11}$  G. Remaining line key as in Fig. 4.

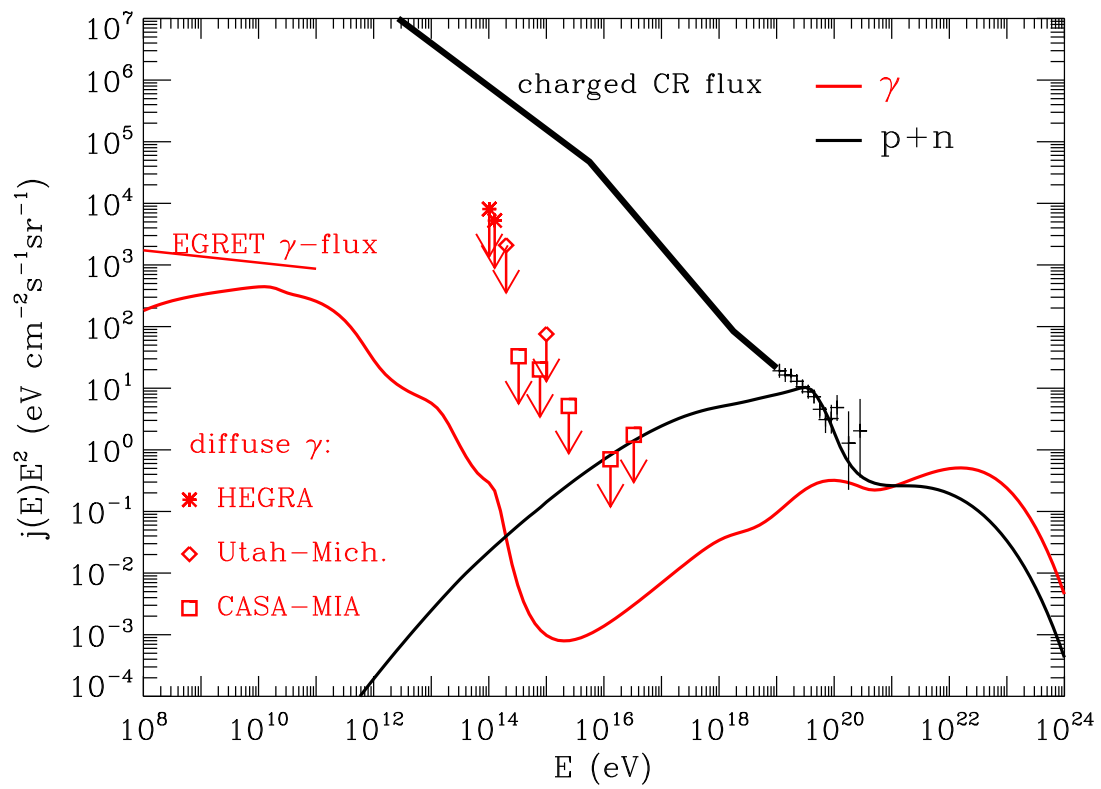


Figure 7: Same as Fig. 6, but for an EGMF of  $10^{-9}$  G.

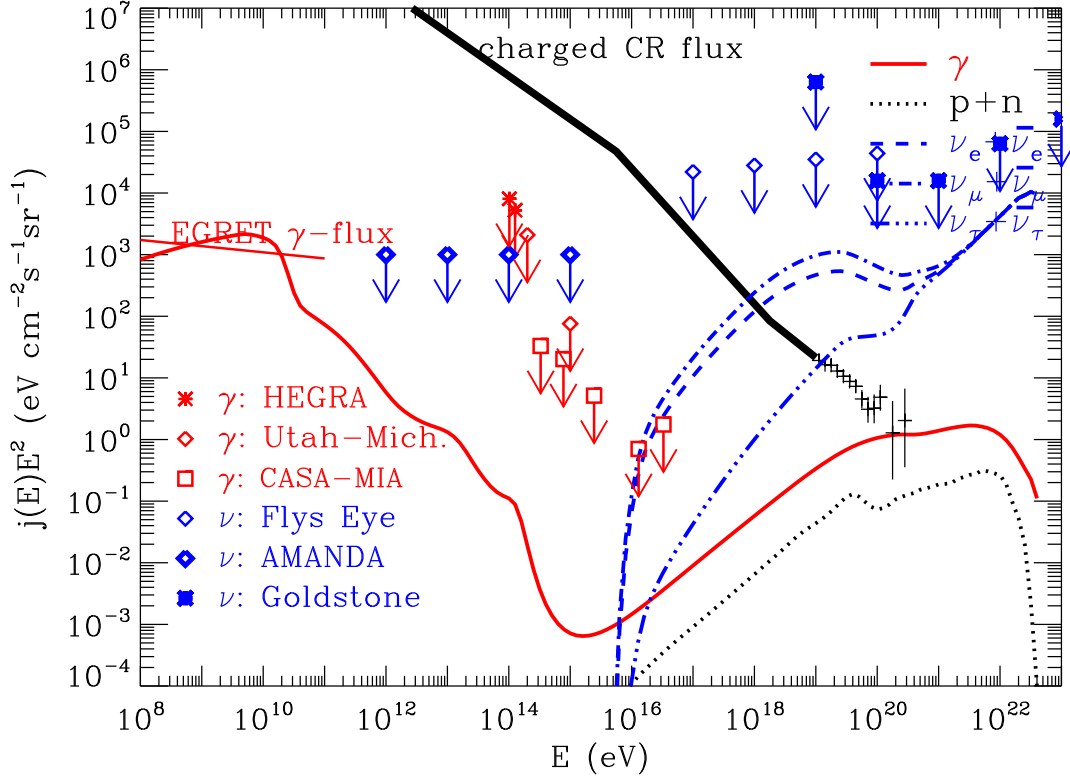


Figure 8: Flux predictions for a TD model characterized by  $p = 1$ ,  $m_X = 10^{14}$  GeV, with X particles exclusively decaying into neutrino-antineutrino pairs of all flavors (with equal branching ratio), assuming neutrino masses  $m_{\nu_e} = 0.1$  eV,  $m_{\nu_\mu} = m_{\nu_\tau} = 1$  eV. For neutrino clustering, an overdensity of  $\simeq 50$  over a scale of  $l_\nu \simeq 5$  Mpc was assumed. The calculation assumed an intermediate URB estimate from Ref. [83] and an EGMF  $\ll 10^{-11}$  G. The line key is as in Fig. 4.